

1 **Competition alters predicted forest carbon cycle responses to nitrogen availability and**
2 **elevated CO₂: simulations using an explicitly competitive, game-theoretic vegetation**
3 **demographic model**

4
5 Ensheng Weng^{1,2}, Ray Dybzinski³, Caroline E. Farrior⁴, Stephen W. Pacala⁵

6 ¹Center for Climate Systems Research, Columbia University, New York, NY 10025

7 ²NASA Goddard Institute for Space Studies, 2880 Broadway, New York, NY 10025

8 ³Institute of Environmental Sustainability, Loyola University Chicago, Chicago, IL 60660

9 ⁴Department of Integrative Biology, University of Texas at Austin, Austin, TX 78712

10 ⁵Department of Ecology & Evolutionary Biology, Princeton University, Princeton, NJ 08544

11

12 **Corresponding author:** Ensheng Weng (wengensheng@gmail.com; phone: 212-678-5585)

13

14 **Key words:** Allocation; Biome Ecological strategy simulator (BiomeE); Competitively-optimal
15 strategy; Game theory; Nitrogen cycle

16

17 **Abstract:** Competition is a major driver of carbon allocation to different plant tissues (e.g.
18 wood, leaves, fine roots), and allocation, in turn, shapes vegetation structure. To improve their
19 modeling of the terrestrial carbon cycle, many Earth system models now incorporate vegetation
20 demographic models (VDMs) that explicitly simulate the processes of individual-based
21 competition for light and soil resources. Here, in order to understand how these competition
22 processes affect predictions of the terrestrial carbon cycle, we simulate forest responses to
23 elevated atmospheric CO₂ concentration [CO₂] along a nitrogen availability gradient using a
24 VDM that allows us to compare fixed allocation strategies versus competitively-optimal
25 allocation strategies. Our results show that competitive and fixed strategies predict opposite
26 fractional allocation to fine roots and wood, though they predict similar changes in total NPP
27 along the nitrogen gradient. The competitively-optimal allocation strategy predicts decreasing
28 fine root and increasing wood allocation with increasing nitrogen, whereas the fixed strategy
29 predicts the opposite. Although simulated plant biomass at equilibrium increases with nitrogen
30 due to increases in photosynthesis for both allocation strategies, the increase in biomass with
31 nitrogen is much steeper for competitively-optimal allocation due to its increased allocation to
32 wood. The qualitatively opposite fractional allocation to fine roots and wood of the two
33 strategies also impacts the effects of elevated [CO₂] on plant biomass. Whereas the fixed
34 allocation strategy predicts an increase in plant biomass under elevated [CO₂] that is
35 approximately independent of nitrogen availability, competition leads to higher plant biomass
36 response to elevated [CO₂] with increasing nitrogen availability. Our results indicate that the
37 VDMs that explicitly include the effects of competition for light and soil resources on allocation
38 may generate significantly different ecosystem-level predictions of carbon storage than those that
39 use fixed strategies.

40

41 **1 Introduction**

42 Allocation of assimilated carbon to different plant tissues is a fundamental aspect of plant growth
43 and profoundly affects terrestrial ecosystem biogeochemical cycles (Cannell and Dewar, 1994;
44 Lacoïnte, 2000). Ecologically, allocation represents an evolutionarily-honed “strategy” of plants
45 that use limited resources and compete with other individuals and consequently drives
46 successional dynamics and vegetation structure (De Kauwe et al., 2014; DeAngelis et al., 2012;
47 Haverd et al., 2016; Tilman, 1988). Biogeochemically, allocation links plant physiological
48 processes, such as photosynthesis and respiration, to biogeochemical cycles and carbon storage
49 of ecosystems (Bloom et al., 2016; De Kauwe et al., 2014). Thus, correctly modeling allocation
50 patterns is critical for correctly predicting terrestrial carbon cycles and Earth system dynamics.

51 In current Earth System Models (ESMs), the terrestrial carbon cycle is usually simulated by
52 pool-based compartment models that simulate ecosystem biogeochemical cycles as lumped pools
53 and fluxes of plant tissues and soil organic matter (Fig. 1: A) (Emanuel and Killough, 1984;
54 Eriksson, 1971; Parton et al., 1987; Randerson et al., 1997; Sitch et al., 2003). In these models,
55 the dynamics of carbon can be described by a linear system of equations (Koven et al., 2015;
56 Luo et al., 2001; Luo and Weng, 2011; Sierra and Mueller, 2015; Xia et al., 2013):

$$57 \frac{dx}{dt} = AX + BU \quad (\text{Eq. 1})$$

58 where X is a vector of ecosystem carbon pools, U is carbon input (i.e., Gross Primary Production,
59 GPP), B is the vector of allocation parameters to autotrophic respiration and plant carbon pools
60 (e.g., leaves, stems, and fine roots), and A is a matrix of carbon transfer and turnover. In this
61 system, carbon dynamics are defined by carbon input (U), allocation (B), and residence time and
62 transfer coefficients (A). The allocation schemes (B) are thus embedded in a linear system, or

63 quasi-linear system if the allocation parameters in B are a function of carbon input (U) or plant
 64 carbon pools (X).

65 The modeling of allocation in this system (i.e., the parameters in vector B) is usually based
 66 on plant allometry, biomass partitioning, and resource limitation (De Kauwe et al., 2014;
 67 Montané et al., 2017). The allocation parameters are either fixed ratios to leaves, stems, and
 68 roots, which may vary among plant functional types (e.g., CENTURY, Parton et al., 1987; TEM,
 69 Raich et al., 1991; CASA, Randerson et al., 1997) or are responsive to climate and soil
 70 conditions as a way to phenomenologically mimic the shifts in allocation that are empirically
 71 observed or hypothesized (e.g., CTEM, Arora and Boer, 2005; ORCHIDEE, Krinner et al., 2005;
 72 LPJ, Sitch et al., 2003). These modeling approaches either assume that vegetation is equilibrated
 73 (fixed ratios) or average the responses of plant types to changes in environmental conditions as a
 74 collective behavior. Thus, the carbon dynamics in these models can be constrained by selecting
 75 appropriate parameters of allocation, turnover rates, and transfer coefficients to fit the
 76 observations (Friend et al., 2007; Hoffman et al., 2017; Keenan et al., 2013).

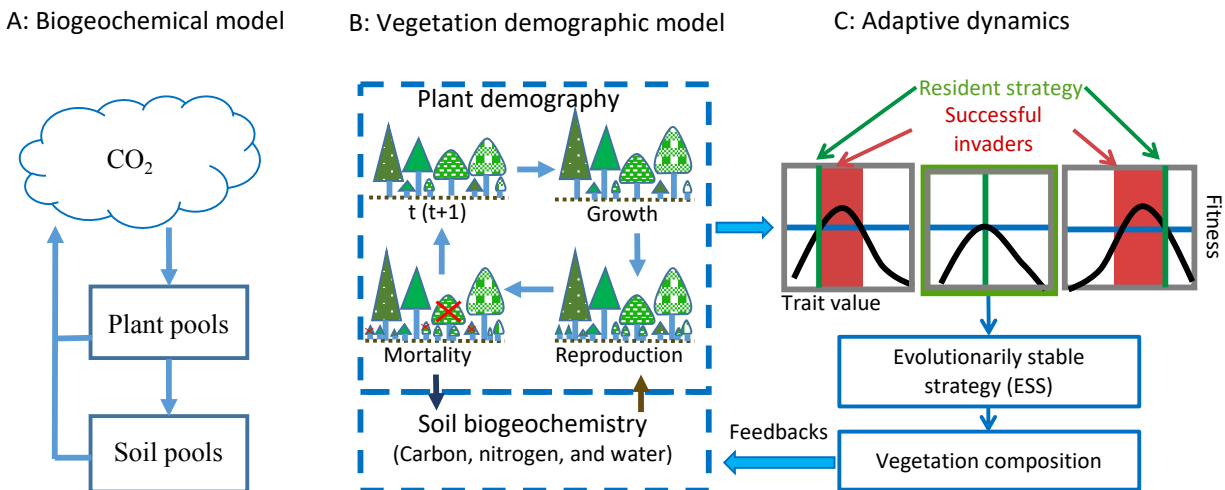


Figure 1 Hierarchical structure of vegetation models

80 To predict transient changes in vegetation structure and composition in response to climate
81 change, vegetation demographic models (VDMs) that are able to simulate transient population
82 dynamics are being incorporated into ESMs (Fisher et al., 2018; Scheiter and Higgins, 2009).
83 Generally, VDMs explicitly simulate demographic processes, such as plant reproduction, growth,
84 and mortality, to generate the dynamics of populations (Fig. 1: B). To speed computations and
85 minimize complexity, groups of individuals are usually modeled as cohorts. With multiple
86 cohorts and PFTs, VDMs can bring plant functional diversity and adaptive dynamics into the
87 system when explicitly simulating individual-based competition for different resources and
88 vegetation succession and thus predict dominant plant traits changes with environmental
89 conditions and ecosystem development (Scheiter et al., 2013; Scheiter and Higgins, 2009; Weng
90 et al., 2015).

91 The combinations of plant traits represent the competition strategies at different stages of
92 ecosystem development. Evolutionarily, a strategy that can outcompete all other strategies in the
93 environment created by itself will be dominant. This strategy is called an evolutionarily stable
94 strategy or a competitively-optimal strategy (McGill and Brown, 2007). In VDMs,
95 competitively-optimal strategies can therefore be reasonably predicted based on the costs and
96 benefits of different strategies (i.e., combinations of plant traits) through their effects on
97 demographic processes (i.e., fitness) and ecosystem biogeochemical cycles (Fig. 1:C) (e.g.,
98 Farris et al., 2015; Weng et al., 2015).

99 The dynamics of plant traits can substantially change predictions of ecosystem
100 biogeochemical dynamics since they change the key parameters of vegetation physiological
101 processes and soil organic matter decomposition (e.g., Dybzinski et al., 2015; Farris et al.,
102 2015; Weng et al., 2017). Therefore, the key parameters that are used to estimate carbon

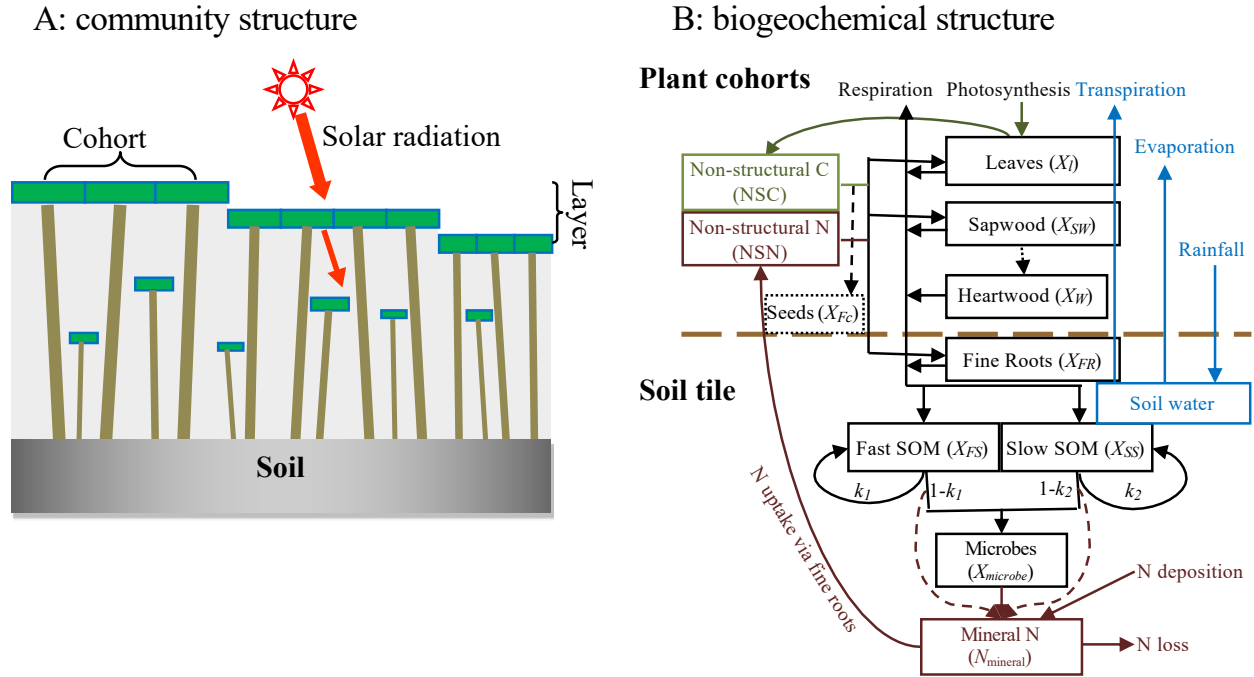
103 dynamics in the linear system model (Eq. 1), such as allocation (B) and residence times in
104 different carbon pools (matrix A , which includes coefficients of carbon transfer and turnover
105 time) become functions of competition strategies that vary with environment and carbon input. In
106 addition, the turnover of vegetation carbon pools becomes a function of allocation, leaf
107 longevity, fine root turnover, and tree mortality rates, which change with vegetation succession
108 and the most competitive plant traits. These changes make the system nonlinear and can lead to
109 large biases within the framework of the compartmental pool-based models as represented by Eq.
110 (1) (Sierra et al., 2017; Sierra and Mueller, 2015). Because of the high complexity associated
111 with demographic and competition processes, the model predictions are usually sensitive to the
112 parameters in these processes and are of high uncertainty (e.g., Pappas et al., 2016).

113 In contrast to their implementation in the more complicated VDMs discussed above,
114 models of competitively-dominant plant strategies using much simpler model structures and
115 assumptions can sometimes be solved analytically (Dybzinski et al., 2011, 2015; Farrior et al.,
116 2013, 2015). Although simplified, such models can pin-point the key processes that improve the
117 predictive power of simulation models (Dybzinski et al., 2011; Farrior et al., 2013, 2015),
118 allowing them to help researchers formulate model processes and understand the simulated
119 ecosystem dynamics in ESMs. For example, the analytical model derived by Farrior et al. (2013)
120 that links interactions between ecosystem carbon storage, allocation, and water stress at elevated
121 atmospheric CO₂ concentration [CO₂] sheds light on the otherwise inscrutable processes leading
122 to varied soil water dynamics in a land model coupled with an VDM (Weng et al., 2015).
123 Recognizing the benefit, Weng et al. (2017) included both a simplified analytical model and a
124 more complicated VDM to understand competitively optimal leaf mass per area, competition
125 between evergreen and deciduous plant functional types, and the resulting successional patterns.

126 In this study, we use a stand-alone simulator derived from the LM3-PPA model (Weng et
127 al., 2017, 2015) to show how forests respond to elevated [CO₂] and nitrogen availability via
128 different competitively-optimal allocation strategies. The demographic processes of this model
129 have been coupled into the land model of the Geophysical Fluid Dynamical Laboratory's Earth
130 System Model (Shevliakova et al., 2009; Weng et al., 2015) and are being added to NASA
131 Goddard Institute for Space Study's Earth system model, ModelE (Schmidt et al., 2014). Using
132 this model, we simulate the shifts in competitively optimal allocation strategies in response to
133 elevated [CO₂] at different nitrogen levels based on insights from the analytical model derived by
134 Dybzinski et al. (2015). Dybzinski et al.'s (2015) model predicts that increases in carbon storage
135 at elevated [CO₂] relative to storage at ambient [CO₂] are largely independent of total nitrogen
136 because of an increasing shift in carbon allocation from long-lived, low-nitrogen wood to short-
137 lived, high-nitrogen fine roots under elevated [CO₂] with increasing nitrogen availability. Here,
138 we analyze the simulated ecosystem carbon cycle variables (gross and net primary production,
139 allocation, and biomass) of separate mono- and polyculture model runs. In the monoculture runs,
140 ecosystem properties are the result of the prescribed allocation strategies of a given PFT. In the
141 polyculture runs, competition between the different allocation strategies results in succession and
142 the eventual dominance of the most competitive allocation strategy for a given nitrogen
143 availability and [CO₂] level. Since everything else in the model is identical, we are able to
144 compare the predictions of single **fixed strategies** with **competitively-optimal allocation**
145 **strategies** by comparing the ecosystem properties of these two types of runs.

146 **2 Methods and Materials**

147 **2.1 BiomeE model overview**



148

149

Figure 2. Structure of BiomeE

150 Panel A: vegetation structure: trees organize their crowns into canopy layers according to both
 151 their height and their crown area following the rules of the PPA model, which mechanistically
 152 models light competition. Panel B: Biogeochemical structure and compartmental pools. The
 153 green, brown, and black lines are the flows of carbon, nitrogen, and coupled carbon and nitrogen,
 154 respectively. The green box is for carbon only. The brown boxes are nitrogen pools. The black
 155 boxes are for both carbon and nitrogen pools, where X can be C (carbon) and N (nitrogen). The
 156 C:N ratios of leaves, fine roots, seeds, and microbes are fixed. The C:N ratios of woody tissues,
 157 fast soil organic matter (SOM), and slow SOM are flexible. Only one tree's C and N pools are
 158 shown in this figure. The blue box and arrows are for water storage in soil and fluxes of rainfall,
 159 evaporation, and transpiration. The model can have multiple cohorts of trees, which share the
 160 same pool structure. The dashed line separates the aboveground and belowground processes.

161

162 We used a stand-alone ecosystem simulator (Biome Ecological strategy simulator,
163 BiomeE) to conduct simulation experiments. BiomeE is derived from the version of LM3-PPA
164 used in Weng *et al.* (2017), and its code is available at Github
165 (<https://github.com/wengensheng/BiomeESS>). In this version, we simplified the processes of
166 energy transfer and soil water dynamics of LM3-PPA (Weng *et al.*, 2015) but still retained the
167 key features of plant physiology and individual-based competition for light, soil water, and, via
168 the decomposition of soil organic matter, nitrogen (Fig. 2 and Supplementary Information I for
169 details). In this model, individual trees are represented as sets of cohorts of similar size trees and
170 are arranged in different vertical canopy layers according to their height and crown area
171 following the rules of the Perfect Plasticity Approximation (PPA) model (Strigul *et al.*, 2008).
172 Sunlight is partitioned into these canopy layers according to Beer's law. Thus, a key parameter
173 for light competition, critical height, is defined; all the trees above this context-dependent height
174 get full sunlight and all trees below this height are shaded by the upper layer trees.

175 Each tree consists of seven pools: leaves, fine roots, sapwood, heartwood, fecundity
176 (seeds), and non-structural carbohydrates and nitrogen (NSC and NSN, respectively) (Fig. 2: b).
177 The carbon and nitrogen in plant pools enter the soil pools with the mortality of individual trees
178 and the turnover of leaves and fine roots. There are three soil organic matter (SOM) pools for
179 carbon and nitrogen: fast-turnover, slow-turnover, and microbial pools, along with a mineral
180 nitrogen pool for mineralized nitrogen in soil. The simulation of SOM decomposition and
181 nitrogen mineralization is based on the models of Gerber *et al.* (2010) and Manzoni *et al.* (2010)
182 and described in detail in Weng *et al.* (2017). The decomposition rate of a SOM pool is
183 determined by the basal turnover rate together with soil temperature and moisture. The nitrogen
184 mineralization rate is a function of decomposition rate and the C:N ratio of the SOM. Microbes

185 must consume more carbon in the high C:N ratio SOM pools to get enough nitrogen and must
 186 release excessive nitrogen in the low C:N ratio SOM pools to get enough carbon for energy
 187 (Weng *et al.* 2017).

188

189

Table 1 Model parameters

Symbol	Definition	Unit	Default value	Reference
α_Z	Parameter of tree height	m m ^{-0.5}	36	Farrior et al., 2013
θ_Z	Diameter exponent of tree height	-	0.5	Farrior et al., 2013
Λ	Taper factor	-	0.75	Weng et al. 2015
ρ_W	Wood density	Kg C m ⁻³	300	Jenkins et al., 2003
α_C	Parameter of crown area	m m ^{-1.5}	150	Farrior et al., 2013
θ_C	Diameter exponent of crown area	-	1.5	Farrior et al., 2013
l^*	Target crown leaf area layers (crown leaf area index)	m ² m ⁻²	3.5	-
σ	Leaf mass per unit area	kg C m ⁻²	0.14	Wright et al., 2004
γ	Specific root area, calculated from root radius and density	m ² kg C ⁻¹	34.5	Pregitzer et al., 2002
φ_{RL}	Ratio of target fine root area to target leaf area	m ² m ⁻²	Varied with PFTs	-
α_{CSA}	ratio of target sapwood cross-sectional area to target leaf area	m ² m ⁻²	0.2x10 ⁻⁴	McDowell et al., 2002
$f_{U,max}$	Maximum mineral nitrogen absorption rate	hour ⁻¹	0.5	-
K_{FR}	Root biomass at which the N-uptake rate is half of the maximum	kg C m ⁻²	0.3	-
$CN_{L,0}$	Target C:N ratio of leaves	kg C kgN ⁻¹	76.5 (Function of LMA)	Wright et al., 2004
$CN_{FR,0}$	Target C:N ratio of fine roots	kg C kgN ⁻¹	60	Magill et al., 2004
$CN_{W,0}$	Target C:N ratio of wood	kg C kgN ⁻¹	350	Martin et al., 2015
$CN_{F,0}$	Target C:N ratio of seeds	kg C kgN ⁻¹	20	Soriano et al., 2011
f_1	Supply rate of NSC and NSN at normal growth	-	1/(3*365)	-
f_2	Maximum fraction of NSC and NSN used for growth in a day	-	0.02	-
$f_{LFR,max}$	Maximum fraction of available carbon allocated to leaves and fine roots	-	0.85	-
ν	Fraction of carbon converted to seeds	-	0.1	-

$r_{D/S}$	Nitrogen-limiting factor	-	Solved by the model (Eqs 9 and 10)
-----------	--------------------------	---	------------------------------------

190

191

192

193

194

195

196

197

198

199

200

201

Plant growth and reproduction are driven by the carbon assimilation of leaves via photosynthesis, which is in turn dependent on water and nitrogen uptake by fine roots. The photosynthesis model is identical to that of LM3-PPA (Weng et al., 2015), which is a simplified version of Leuning model (Leuning et al., 1995). This model first calculates photosynthesis rate, stomatal conductance, and water demand of the leaves of each tree (cohort) in the absence of soil water limitation. Then, it calculates available water supply as a function of fine root surface area and soil water content. The demand-based assimilation rate and stomatal conductance are adjusted if soil water supply is less than plant water demand. Soil water content is calculated based on the fluxes of precipitation, soil surface evaporation, and plant water update (transpiration) in three layers of soil to a depth of 2 meters. (Please see Supplementary Information I for details).

202

203

204

205

206

Assimilated carbon enters into the NSC pool and is subsequently used for respiration, growth, and reproduction. Empirical allometric equations relate woody biomass (including coarse roots, bole, and branches), crown area, and stem diameter. The individual-level dimensions of a tree, *i.e.*, height (Z), biomass (S), and crown area (A_{CR}) are given by empirical allometries (Dybzinski et al., 2011; Farrior et al., 2013):

$$\begin{aligned}
 Z(D) &= \alpha_Z D^{\theta_Z} \\
 S(D) &= 0.25\pi\lambda\rho_W\alpha_Z D^{2+\theta_Z} \\
 A_{CR}(D) &= \alpha_c D^{\theta_c}
 \end{aligned}
 \tag{Eq. 2}$$

207

208

where Z is tree height, D is tree diameter, S is total woody biomass carbon (including bole, coarse roots, and branches) of a tree, α_c and α_Z are PFT-specific constants, $\theta_c=1.5$ and $\theta_Z=0.5$

209 (Farrior et al., 2013) (although they could be made PFT-specific if necessary), π is the circular
 210 constant, λ is a PFT-specific taper constant, and ρ_w is PFT-specific wood density (kg C m^{-3})
 211 (Table 1).

212 We set *targets* for leaf (L^*), fine root (FR^*), and sapwood cross-sectional area (A_{SW}^*) that
 213 govern plant allocation of non-structural carbon and nitrogen during growth. These *targets* are
 214 related by the following equations based on the assumption of the pipe model (Shinozaki,
 215 Kichiro et al., 1964):

$$\begin{aligned}
 L^*(D, p) &= l^* \cdot A_{CR}(D) \cdot \sigma \cdot p(t) \\
 FR^*(D) &= \varphi_{RL} \cdot l^* \cdot \frac{A_{CR}(D)}{\gamma} \\
 A_{SW}^*(D) &= \alpha_{CSA} \cdot l^* \cdot A_{CR}(D)
 \end{aligned}
 \tag{Eq. 3}$$

216 where $L^*(D, p)$, $FR^*(D)$, and $A_{SW}^*(D)$ are the targets of leaf mass (kg C/tree), fine root biomass
 217 (kg C/tree), and sapwood cross sectional area (m^2/tree), respectively, at tree diameter D ; l^* is the
 218 target leaf area per unit crown area of a given PFT; $A_{CR}(D)$ is the crown area of a tree with
 219 diameter D ; σ is PFT-specific leaf mass per unit area (LMA); and $p(t)$ is a PFT-specific function
 220 ranging from zero to one that governs leaf phenology (Weng et al., 2015); φ_{RL} is the target ratio
 221 of total root surface area to the total leaf area; γ is specific root area; and α_{CSA} is an empirical
 222 constant (the ratio of sapwood cross-sectional area to target leaf area). The phenology function
 223 $p(t)$ takes values 0 (non-growing season) or 1 (growing season) following the phenology model
 224 of LM3-PPA (Weng et al., 2015). The onset of a growing season is controlled by two variables,
 225 growing degree days (GDD), and a weighted mean daily temperature (T_{pheno}), while the end of a
 226 growing season is controlled by T_{pheno} . (Please see Supplementary Information I for details of the
 227 phenology model)

228 **Nitrogen uptake**

229 The rate of nitrogen uptake (U , g N m⁻² hour⁻¹) from the soil mineral nitrogen pool is an
 230 asymptotically increasing function of fine root biomass density ($C_{FR,total}$, kg C m⁻²), following
 231 McMurtrie *et al.* (2012)

$$U = f_{U,max} \cdot N_{mineral} \cdot \frac{C_{FR,total}}{C_{FR,total} + K_{FR}}, \quad (\text{Eq. 4})$$

232 where, $N_{mineral}$ is the mineral nitrogen in soil (g N m⁻²), $f_{U,max}$ is the maximum rate of nitrogen
 233 absorption per hour when $C_{FR,total}$ approaches infinity, K_{FR} is a shape parameter (kg C m⁻²) at
 234 which the nitrogen uptake rate is half of the parameter $f_{U,max}$. The nitrogen uptake rate of an
 235 individual tree (U_{tree} , kg N hour⁻¹ tree⁻¹) is calculated as follows:

$$U_{tree} = U \cdot \frac{C_{FR,tree}}{C_{FR,total}}, \quad (\text{Eq. 5})$$

236 where, $C_{FR,tree}$ is the fine root biomass of a tree (kg C tree⁻¹). The nitrogen absorbed by roots
 237 enters into the NSN pool and then is allocated to plant tissues through plant growth.

238 **Allocation and plant growth**

239 The partitioning of carbon and nitrogen into the plant pools (*i.e.*, leaves, fine roots, and
 240 sapwood) is limited by the allometric equations, targets of leaves, fine roots, and sapwood cross-
 241 sectional area, and the stoichiometry (*i.e.*, C:N ratios) of these plant tissues. At a daily time step,
 242 the model calculates the amount of carbon and nitrogen that are available for growth according
 243 to the total NSC and NSN and current leaf and fine root biomass. Basically, the available NSC
 244 (G_C) is the summation of a small fraction (f_1) of the total NSC in an individual plant and the
 245 differences between the targets of leaf and fine roots and their current biomass capped by a larger
 246 fraction (f_2) of NSC (Eq. 6.1). The available NSN (G_N) is analogous to that of the NSC and
 247 meets approximately the stoichiometrical requirement of plant tissues (Eq. 6.2).

$$G_C = \min (f_1 NSC + L^* + FR^* - L - FR, f_2 NSC) \quad (\text{Eq. 6.1})$$

$$G_N = \min (f_1 NSN + N_L^* + N_{FR}^* - N_L - N_{FR}, f_2 NSN) \quad (\text{Eq. 6.2})$$

248 where L^* and FR^* are the targets of leaves and fine roots, respectively (see Eq. 3); L and FR are
 249 current leaf and fine roots biomass, respectively; N_L^* and N_{FR}^* are nitrogen of leaves and fine
 250 roots at their targets according to their target C:N ratios. The parameter f_1 is the fraction of NSC
 251 (or NSN) for normal growth after leaves and fine roots approach their targets and f_2 caps the
 252 maximum daily availability of NSC (or NSN) during the period of leaf flush at the beginning of
 253 a growing season. The parameter f_1 is much smaller than f_2 . We let $f_1 = 1/(365 \times 3)$ and $f_2 = 0.02$ in
 254 this study.

255 The allocation of the available NSC (i.e., G_C) to wood (G_W), leaves (G_L), fine roots (G_{FR}),
 256 and seeds (G_F) follows the equations below (Eq. 7). These equations describe the mass growth of
 257 plant tissues with nitrogen effects on the carbon allocation between high-nitrogen tissues and
 258 low-nitrogen tissues (wood) for maximizing leaves and fine roots growth (G_L and G_{FR} ,
 259 respectively), optimizing carbon usage at given nitrogen supply (G_N), and keeping the tissues at
 260 their target C:N ratios.

$$G_C \geq G_W + G_L + G_{FR} + G_F \quad (\text{Eq. 7.1})$$

$$G_N \geq \frac{G_L}{CN_{L,0}} + \frac{G_{FR}}{CN_{FR,0}} + \frac{G_F}{CN_{F,0}} + \frac{G_W}{CN_{W,0}} \quad (\text{Eq. 7.2})$$

$$\frac{(FR + G_{FR})\gamma}{(L + G_L)/\sigma} = \varphi_{RL} \quad (\text{Eq. 7.3})$$

$$G_L + G_{FR} = \text{Min} \left(\begin{array}{c} L^* + FR^* - L - FR, \\ f_{LFR,max} G_C \end{array} \right) \cdot r_{S/D} \quad (\text{Eq. 7.4})$$

$$G_F = \left[G_C - \text{Min} \left(\frac{L^* + FR^* - L - FR,}{f_{LFR,max} G_C} \right) r_{S/D} \right] \cdot v \cdot r_{S/D} \quad (\text{Eq. 7.5})$$

$$G_W = \left[G_C - \text{Min} \left(\frac{L^* + FR^* - L - FR,}{f_{LFR,max} G_C} \right) r_{S/D} \right] \cdot (1 - v \cdot r_{S/D}) \quad (\text{Eq. 7.6})$$

261 where, $CN_{L,0}$, $CN_{FR,0}$, $CN_{F,0}$, and $CN_{W,0}$ are the target C:N ratios of leaves, fine roots, seeds, and
 262 sapwood, respectively; γ is specific root area ($\text{m}^2 \text{ kg C}^{-1}$); σ is leaf mass per unit area (kg C m^{-2});
 263 $f_{LFR,max}$ is the maximum fraction of G_C for leaves and fine roots (0.85 in this study); v is the
 264 fraction of left carbon for seeds (0.1 in this study); $r_{S/D}$ is a nitrogen-limiting factor ranging from
 265 0 (no nitrogen for leaves, fine roots, and seeds) to 1 (nitrogen available for full growth of leaves,
 266 fine roots, and seeds). The parameter $r_{S/D}$ controls the allocation of G_C and G_N to the four plant
 267 pools (Eq. 7.1). It can be analytically solved (Eqs. 8 and 9).

$$r_{S/D} = \text{Min} \left[1, \text{Max} \left(0, \frac{G_N - G_C / CN_W}{N' - G_C / CN_W} \right) \right], \quad (\text{Eq. 8})$$

268 where, N' is defined as the potential nitrogen demand for plant growth at $r_{S/D}=1$ (i.e., no nitrogen
 269 limitation).

$$N' \equiv \frac{\gamma \sigma \left[FR + \text{Min} \left(\frac{L^* + FR^* - L - FR,}{f_{LFR,max} G_C} \right) \right] - \varphi_{RL} L}{(\gamma \sigma + \varphi_{RL}) CN_L} + \frac{\varphi_{RL} \left[L + \text{Min} \left(\frac{L^* + FR^* - L - FR,}{f_{LFR,max} G_C} \right) \right] - \gamma \sigma L}{(\gamma \sigma + \varphi_{RL}) CN_{FR}} + \quad (\text{Eq. 9})$$

$$\frac{v \left[G_C - \text{Min} \left(\frac{L^* + FR^* - L - FR,}{f_{LFR,max} G_C} \right) \right]}{CN_F} + \frac{(1-v) \left[G_C - \text{Min} \left(\frac{L^* + FR^* - L - FR,}{f_{LFR,max} G_C} \right) \right]}{CN_W}.$$

270 When $G_N \geq N'$ ($r_{S/D} = 1$), there is no nitrogen limitation, and all the G_C will be used for plant
 271 growth and the allocation follows the rules of the carbon only model (Eqs 7.4~7.6 as $r_{S/D} = 1$).
 272 The excessive nitrogen ($G_N - N'$) will be returned to the NSN pool (as if they were never taken
 273 out). When $G_C / CN_{W,0} < G_N < N'$ (i.e., $0 < r_{S/D} < 1$), all G_C and G_N will be used in new tissue growth;
 274 however, the leaves and fine roots cannot reach their targets at this step (i.e. they are down-

275 regulated). When $G_N \leq G_C / CN_{W,0}$ ($r_{S/D} = 0$), all the G_N will be allocated to sapwood and the
 276 excessive carbon ($G_C - G_N CN_{W,0}$) will be returned to NSC pool. This is a very rare case since a
 277 low G_N leads to low leaf growth, reducing G_C before the case $G_N < G_C / CN_{W,0}$ happens. Therefore,
 278 in most cases, Eq. 7.1 is: $G_C = G_W + G_L + G_{FR} + G_F$. Overall, this strategy down-regulates leaf
 279 production under low nitrogen conditions while making use of assimilated carbon in height-
 280 structured competition for light.

281 Allocation to wood tissues (G_W) drives the growth of tree diameter, height, and crown
 282 area and thus increases the targets of leaves and fine roots (Eq. 3). By differentiating the stem
 283 biomass allometry in Eq. 2 with respect to time, using the fact that dS/dt equals the carbon
 284 allocated for wood growth (G_W), we have the diameter growth:

$$\frac{dD}{dt} = \frac{G_W}{0.25\pi\Lambda\rho_w\alpha_z(2+\theta_z)D^{1+\theta_z}} \quad (\text{Eq. 10})$$

285 This equation transforms the mass growth to structural changes in tree architecture. With an
 286 updated tree diameter, we can calculate the new tree height and crown area using allometry
 287 equations (Eq. 2) and targets of leaf and fine root biomass (Eq. 3) for the next growth step.

288 Overall, this is a flexible allocation scheme and still follows the major assumptions in the
 289 previous version of LM3-PPA (Weng, et al., 2015, 2017). This allocation scheme prioritizes the
 290 allocation to leaves and fine roots, maintains a minimum growth rate of stems, and keeps the
 291 constant area ratio of fine roots to leaves. Based on these allocation rules, the average allocation
 292 of carbon and nitrogen to leaves, fine roots, and wood over a growing season are governed by the
 293 targets for the leaf area per unit crown area (i.e., crown leaf area index, l^*) and fine root area per
 294 unit leaf area (ϕ_{RL}). Since the crown leaf area index, l^* , is fixed in this study, ϕ_{RL} is the key
 295 parameter determining the relative allocation of carbon to fine roots and stems. A high ϕ_{RL}

296 means a high relative allocation to fine roots and therefore low relative allocation to stems, and
297 *vice versa*. Note, here ϕ_{RL} is fixed for each PFT and will remain so for all the model runs.

298 The process of choosing a context-dependent competitively dominant ϕ_{RL} will take place
299 after finding the fitness of each ϕ_{RL} in monoculture and in competition with other PFTs (*i.e.*,
300 different values of ϕ_{RL}). The competitively optimal strategy is the one that can successfully
301 exclude all others in the processes of competition and succession, but it is not necessarily the one
302 that maximizes production in monoculture. For example, each ϕ_{RL} creates an environment of
303 light profile and soil nitrogen in its monoculture. Other ϕ_{RL} PFTs may have higher fitness in this
304 environment than the one that creates it. Only the competitively dominant strategy has the
305 highest fitness in the environment it creates (Fig. 1: C).

306 **2.2 Site and Data**

307 Data pertaining to vegetation, climate, and soil at Harvard Forest (Aber et al., 1993; Hibbs, 1983;
308 Urbanski et al., 2007) were used to design the plant functional types (PFTs) and ecosystem
309 nitrogen levels used in the simulation experiments, to drive the model, and to calibrate model
310 parameters. Harvard Forest is located in Massachusetts, USA (42.54°, -72.17°). The climate of
311 Harvard Forest is cool temperate with annual precipitation 1050 mm, distributed fairly evenly
312 throughout the year. The annual mean temperature is 8.5 °C with a high monthly mean
313 temperature of 20°C in July and a low of -7°C in January. The soils are mainly sandy loam with
314 average depth around 1 m and are moderately well drained in most areas. In forest sites, soil
315 carbon is around 8 kg C m⁻² and nitrogen 300 g N m⁻² (Compton and Boone, 2000). The
316 vegetation is deciduous broadleaf/mixed forest with major species red oak (*Quercus rubra*), red
317 maple (*Acer rubrum*), black birch (*Betula lenta*), white pine (*Pinus strobus*), and hemlock (*Tsuga*
318 *canadensis*) (Compton and Boone, 2000; Savage et al., 2013). The data used to drive our model

319 runs are gap-filled hourly meteorological data at Harvard Forest from 1991 to 2006, obtained
320 from North American Carbon Program (NACP) Site-Level Synthesis datasets (Barr et al., 2013).

321

322 **2.3 Simulation experiments**

323 We set two atmospheric CO₂ concentration ([CO₂]) levels: 380 ppm and 580 ppm, and
324 eight ecosystem total nitrogen levels (ranging from 114.5 g N m⁻² to 552 g N m⁻² at the interval
325 of 62.5 g N m⁻²) by assigning the initial content of the slow SOM pool for our simulation
326 experiments (Table 2). This range covers the soil nitrogen contents across the plots at Harvard
327 Forest with different species compositions and land use history (200~300 g N m⁻²) (Compton and
328 Boone, 2000; Melillo et al., 2011), and represents the range from infertile to fertile soils in
329 temperate forests (Post et al., 1985; Yang et al., 2011). The nitrogen cycles through the plant and
330 soil pools and is redistributed among them via plant demographic processes, soil carbon
331 transfers, and plant uptake. In all the simulation experiments, we assume the ecosystem has no
332 nitrogen inputs and no outputs for convenience since we already have eight total nitrogen levels
333 to represent the consequences of different nitrogen input and output processes at an equilibrium
334 state. The PFTs were based on an evergreen needle-leaved tree PFT with different leaf to fine
335 root area ratios, ϕ_{RL} , in the range from 1 to 8 (Table 2). Simply stated, the PFTs we investigate
336 only differ in parameter ϕ_{RL} .

337 We define the model runs started with only one fixed- ϕ_{RL} PFT as “monoculture runs”
338 although the actual allocation of carbon to different plant tissues varies with [CO₂] and
339 ecosystem nitrogen availability. The model runs started with multiple PFTs are called
340 “polyculture runs” (eight PFTs with different ϕ_{RL} at the beginning, although many are driven to

341 extinction during a given model run). We conducted one set of monoculture runs and two sets of
 342 polyculture runs (Table 2).

343

344

Table 2 Simulation experiments

Type	Model runs	Initial PFT(s) ϕ_{RL}	Ecosystem total nitrogen levels	CO ₂ concentration [CO ₂]
Monoculture runs	One model run per combination of PFT (ϕ_{RL}), nitrogen level, and CO ₂ concentration	One of the following PFTs: $\phi_{RL} = 1, 2, 3, 4, 5, 6, 7, \text{ or } 8$	Eight levels ranging from 114.5 g N m ⁻² to 552 g N m ⁻² at the interval of 62.5 g N m ⁻² : (i.e., 114.5, 177, 239.5, 302, 364.5, 427, 489.5, and 552 g N m ⁻²)	Ambient: 380 ppm Elevated: 580 ppm
Polyculture runs I	One model run per combination of nitrogen level and CO ₂ concentration	All the PFTs ($\phi_{RL} = 1 \sim 8$) used in the monoculture runs		
Polyculture runs II	One model run per combination of nitrogen level and CO ₂ concentration	Eight PFTs with ϕ_{RL} ranging from 4.5-0.5 <i>i</i> to 8.5-0.5 <i>i</i> at the interval of 0.5, where <i>i</i> denotes the eight nitrogen levels from 114.5 to 552 gN m ⁻² .		

345

346 In the monoculture runs, we run the full combinations of eight PFTs with root/leaf area
 347 ratios (ϕ_{RL}) from 1 to 8, eight ecosystem total nitrogen levels, and two CO₂ concentrations (380
 348 ppm and 580 ppm) (Table 2). For the eight PFTs, only those with $\phi_{RL} \leq 6$ survived at ambient
 349 [CO₂] (380 ppm) because the carbon assimilated by leaves could not meet the demand by plant
 350 tissues at $\phi_{RL} > 6$. The monoculture runs are for exploring the model predictions of gross primary
 351 production (GPP), net primary production (NPP), allocation, and biomass at equilibrium with
 352 fixed ϕ_{RL} at different total nitrogen levels.

353 In polyculture runs I, we used the same PFTs as in those monoculture runs, where their φ_{RL}
354 varied from 1 to 8 at the interval of 1.0 and the ecosystem total nitrogen levels were the same as
355 those used in the monoculture runs (Table 2). This set of polyculture runs was used to explore
356 successional patterns at both ambient and elevated $[\text{CO}_2]$ (380 ppm and 580 ppm, respectively).
357 However, this set of model runs could not show the details of equilibrium plant biomass and
358 allocation patterns along the nitrogen gradient because of the large intervals between the φ_{RL}
359 values.

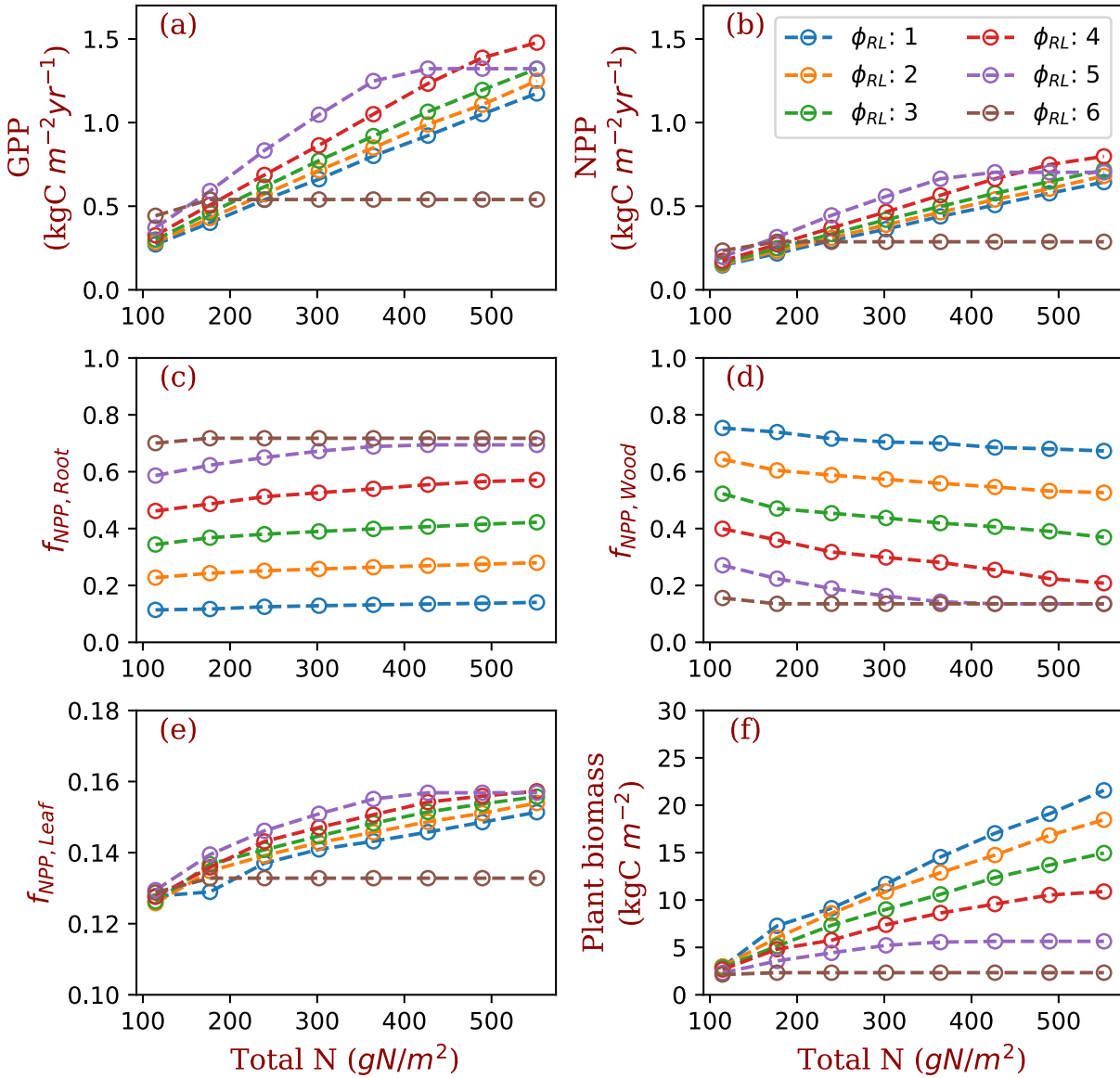
360 To achieve greater resolution in our competition predictions, we designed the polyculture
361 runs II using a dynamic PFT combination scheme according to the ranges of φ_{RL} obtained from
362 the polyculture runs I that could survive at a particular nitrogen level at both CO_2 concentrations.
363 For each nitrogen level, we set eight PFTs with φ_{RL} that varied in a range 3.5 (e.g., $x \sim x+3.5$) at
364 the interval of 0.5, starting with the highest φ_{RL} of 8.0 at the lowest N level (114.5 g N m^{-2}) and
365 decreasing 0.5 per level of increase in ecosystem total N. We used $i=1, 2, \dots, 8$ to denote the
366 eight N levels from 114.5 to 552 g N m^{-2} . The φ_{RL} of the eight PFTs at each level were $5.0-0.5i$,
367 $5.5-0.5i, \dots, 8.5-0.5i$ (Table 2). For example, at the nitrogen of 114.5 g N m^{-2} ($i = 1$), the φ_{RL} of
368 the eight PFTs were 4.5, 5.0, $\dots, 8.0$ and at 177 g N m^{-2} ($i = 2$), they were 4.0, 4.5, $\dots, 7.5$.

369 For both monoculture and polyculture runs, visual inspection indicated that stands had
370 reached equilibrium after ~ 1200 years. To be conservative, we present equilibrium data by
371 averaging model properties between years 1400 and 1800. We compared simulated equilibrium
372 GPP, NPP, allocation (both absolute amount of carbon and fractions of the total NPP), and plant
373 biomass of the polyculture runs II with those from the monoculture runs. We used the results
374 from one PFT ($\varphi_{RL}=4$) to highlight the differences of plant responses with competitively optimal
375 allocation strategies obtained from the polyculture runs II.

376

377 **3 Results**

378 In the monoculture runs, GPP and NPP increase by a factor of three along the gradient of
379 nitrogen used in this study (114.5 - 552 g N m⁻²) at both ambient (Fig. 3) and elevated [CO₂]
380 (Figs. S1). The magnitude of differences in GPP and NPP due to differences in fixed allocation
381 within a given nitrogen level is comparable to the magnitude of differences in GPP and NPP due
382 to nitrogen level within a given fixed allocation strategy (Fig. 3: a and b) when ϕ_{RL} is in the
383 range that allows plants to grow normally (1~5 in the case of ambient [CO₂]). As prescribed by
384 the definition of ϕ_{RL} , allocation of NPP to fine roots increases with ϕ_{RL} in monoculture runs (Fig.
385 3: c). As a consequence, allocation of NPP to wood decreases as ϕ_{RL} increases (Fig. 3: d).
386 Allocation to leaves does not change much with ϕ_{RL} . (Fig. 3: e, note differences in scale).
387 Correspondingly, plant biomass at equilibrium decreases with ϕ_{RL} (Fig. 3: f). The effects of
388 nitrogen on the allocation of carbon to fine roots and wood follow our allocation model
389 assumptions because more carbon is allocated to low-nitrogen woody tissues in our model when
390 nitrogen is limited. However, the amplitude of changes in GPP and NPP induced by nitrogen
391 availability is lower than the amplitude of changes resulting from different values of ϕ_{RL} in the
392 monoculture runs.



393

394 **Figure 3. GPP, NPP, Allocation and Plant biomass at equilibrium state simulated by**

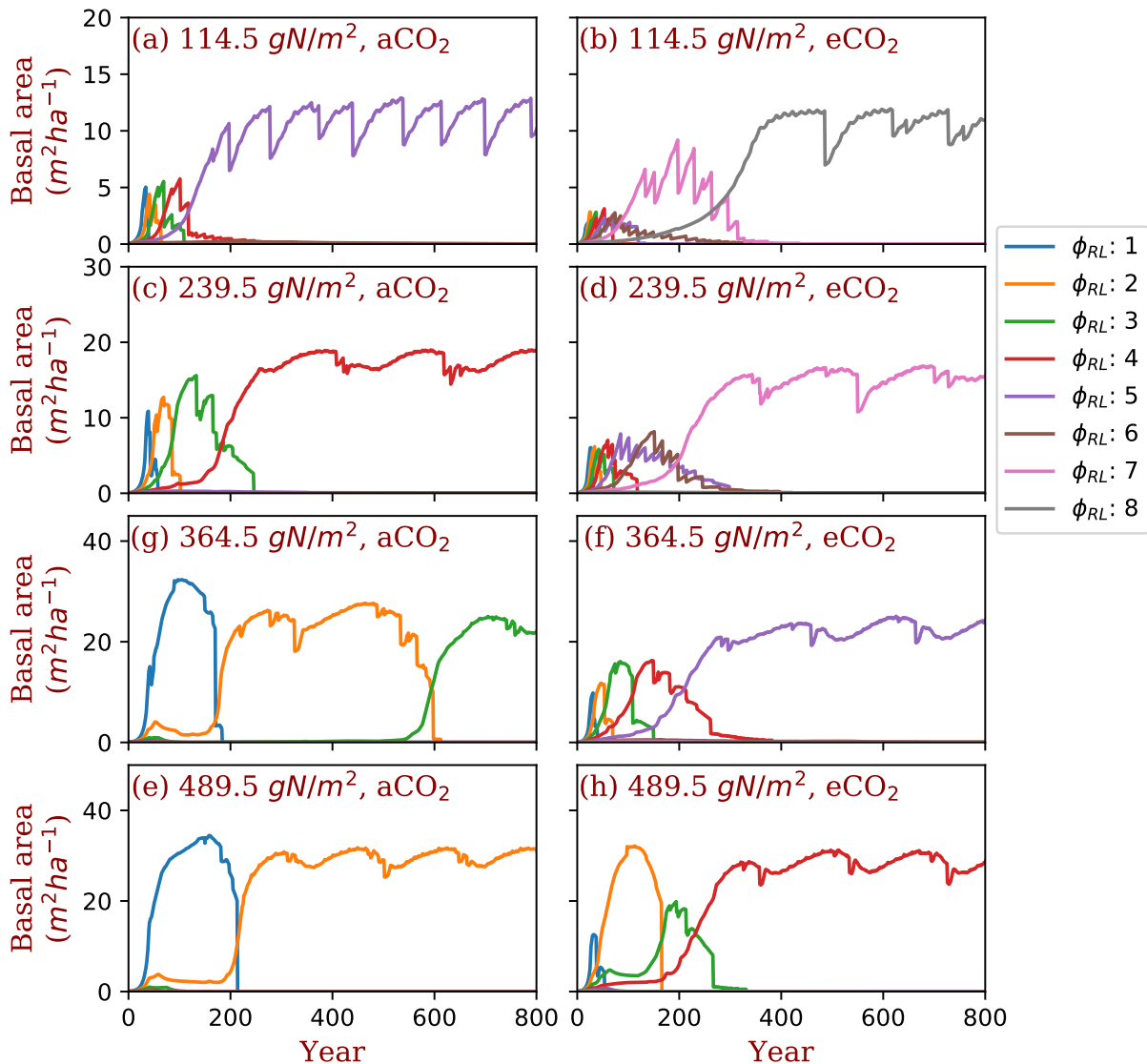
395 **monoculture runs.** GPP: Gross primary production; NPP: Net primary production; $f_{NPP,x}$: the

396 fraction of NPP allocated to x , where x is Root (fine roots), Leaf (leaves in crown), or Wood

397 (including tree trunk, stems, and coarse roots). The data are from the averages of the model run

398 years from 1400 and 1800. Each model run is initiated with one PFT with fixed ratio of fine root

399 area to leaf area (ϕ_{RL}).



401

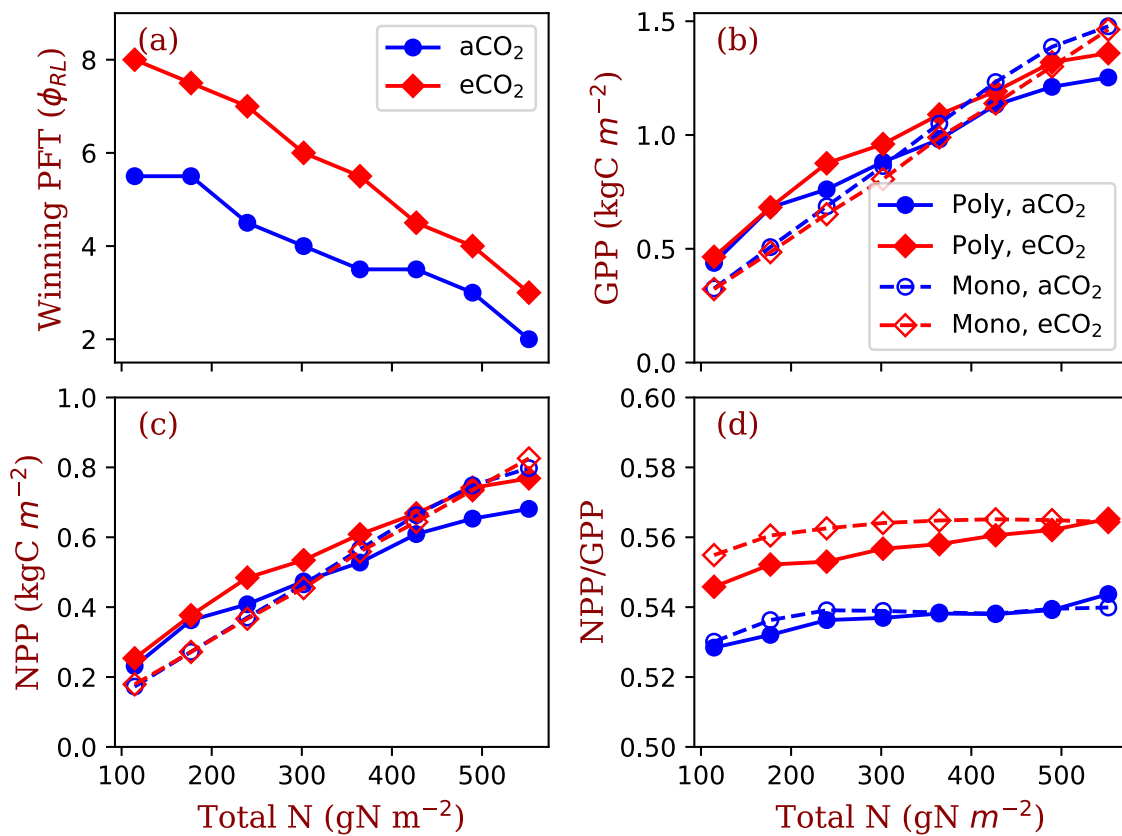
402 **Figure 4 Successional patterns of polyculture runs I at ambient and elevated [CO₂]**
 403 **concentrations.** ϕ_{RL} is the fixed ratio of fine root area to leaf area of a particular strategy.

404

405 We used two sets of polyculture runs to look for the ϕ_{RL} that is closest to competitively
 406 optimal. In the polyculture runs I, where ϕ_{RL} ranges from 1 to 8 at all nitrogen levels, the
 407 winning strategy (ϕ_{RL}) increases from 5 to 2 as the total nitrogen increases from 114.5 g N m⁻² to
 408 489.5 g N m⁻² at ambient [CO₂] (380 ppm) (Fig. 4: a, c, g, e). Elevated [CO₂] (580 ppm) shifts

409 the winning strategy to higher (ϕ_{RL}) at all the total nitrogen levels. As shown in Fig. 4, the
 410 winning strategy shifts from $\phi_{RL}=5$ to $\phi_{RL}=8$ at 114.5 g N m^{-2} and from $\phi_{RL}=2$ to $\phi_{RL}=4$ at 489.5
 411 g N m^{-2} . In some situations (e.g., Fig. 4: g and Figs. S2 and S3), it takes a long time for the most
 412 competitive PFTs to out-compete the previously dominant PFTs because of the sequential
 413 replacement of dominant PFTs during the course of succession and the slow growth rate of trees
 414 in understory.

415



416

417 **Figure 5** Winning PFTs (ϕ_{RL} , a) in polyculture runs II and equilibrium Gross Primary
 418 **Production (GPP, b), Net Primary Production (NPP, c), and Carbon Use Efficiency**
 419 **(NPP/GPP, d) at two CO₂ concentrations (aCO₂: 380 ppm; eCO₂: 580 ppm). The closed**
 420 **symbols with solid line represent polyculture runs. The open symbols with dashed lines represent**

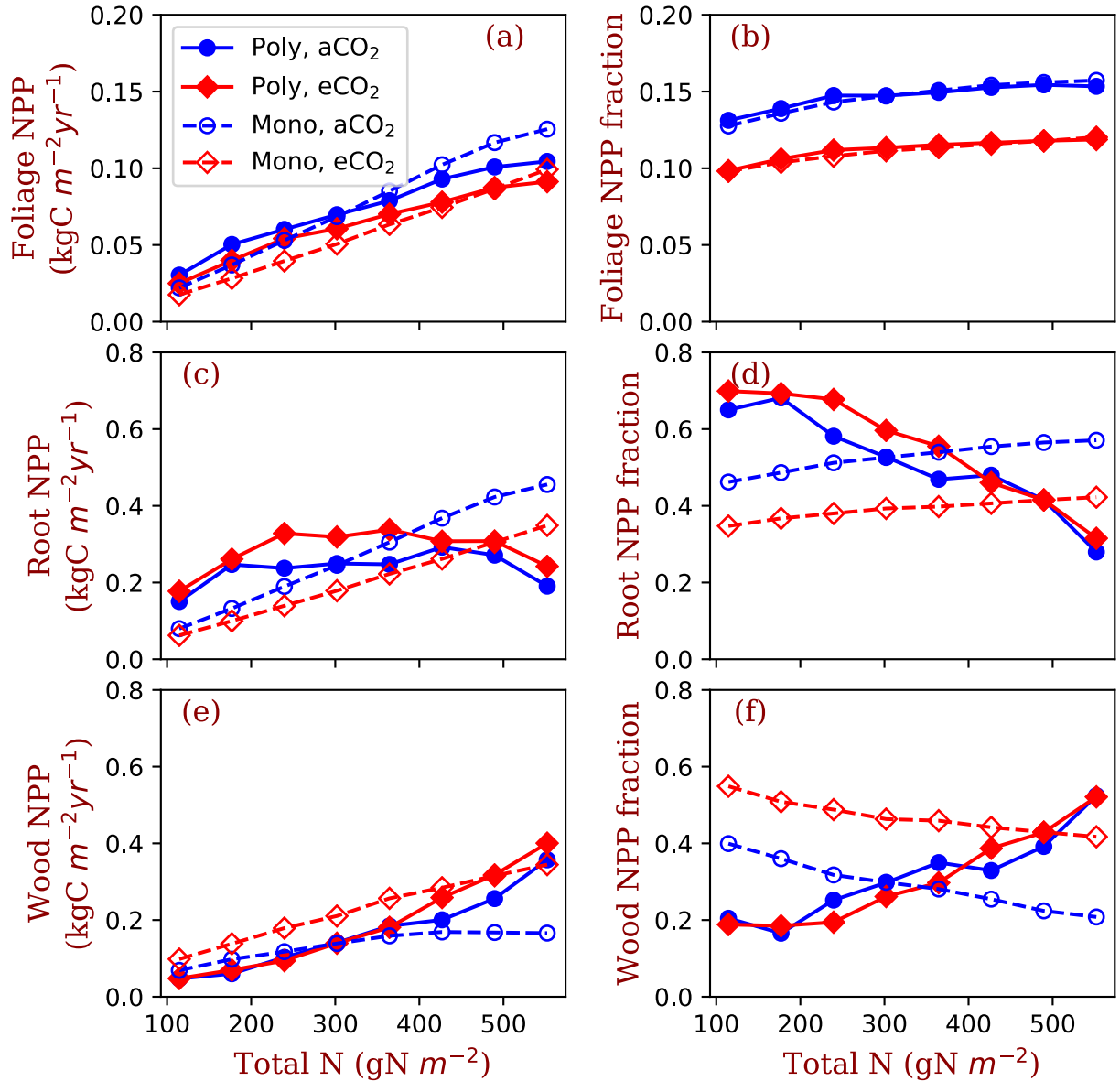
421 monoculture runs (only $\phi_{RL}=4$ shown in this figure). ϕ_{RL} is the fixed ratio of fine root area to leaf
422 area of a particular strategy.

423

424 Based on the shifts of the winning ϕ_{RL} from ambient $[\text{CO}_2]$ to elevated $[\text{CO}_2]$ at the eight
425 nitrogen levels, we designed the polyculture runs II with high resolution of ϕ_{RL} and calculated
426 their GPP, NPP, allocation, and plant biomass at equilibrium state. The of ϕ_{RL} of the winning
427 PFTs decreases from 5.5 to 2 at ambient $[\text{CO}_2]$ and from 8.0 to 3.0 at elevated $[\text{CO}_2]$ as total
428 nitrogen increases from 114.5 g N m⁻² to 552.0 g N m⁻². The equilibrium GPP and NPP increase
429 with total nitrogen at values similar to those of the monoculture runs (Fig. 5: b and c). However,
430 the CO₂ stimulation of NPP increases with total nitrogen in the polyculture runs more than it in
431 the monoculture runs. Elevated $[\text{CO}_2]$ increases carbon use efficiency (defined as the ratio of
432 NPP to GPP in this study, NPP/GPP) in both the monoculture and polyculture runs (Fig. 5: d).
433 Also, the dependence of NPP:GPP ratio on nitrogen is higher in the polyculture runs than it in
434 the monoculture runs (Fig. 5:c).

435 Allocation of NPP to leaves increases with nitrogen in all conditions, i.e. both competition
436 and monoculture at both ambient $[\text{CO}_2]$ and elevated $[\text{CO}_2]$ (Fig. 6: a). Foliage NPP is similar in
437 these four model runs when nitrogen is low. At high nitrogen (>400 g N m⁻²), polyculture runs
438 have higher foliage NPP than the monoculture runs generally. Allocation to leaves is relatively
439 stable across the nitrogen gradient at the two $[\text{CO}_2]$ levels (Fig. 6: b). The fraction of NPP
440 allocated to leaves changes little with nitrogen (Fig. 6: b) and it is universally higher at ambient
441 $[\text{CO}_2]$ than it at elevated $[\text{CO}_2]$.

442



443

444 **Figure 6** Allocation to leaves, fine roots, and wood tissues of the competition and monoculture
 445 runs at the eight total nitrogen levels and two CO₂ concentrations (aCO₂: 380 ppm; eCO₂: 580
 446 ppm). The panels a, c, and e show the NPP allocated to the tissues and the panels b, d, and f
 447 show the fractions of the allocation in total NPP. The closed symbols with solid line represent
 448 polyculture runs (Poly). The open symbols with dashed lines represent monoculture runs (only
 449 $\varphi_{RL}=4$ shown in this figure, Mono). φ_{RL} is the fixed ratio of fine root area to leaf area of a
 450 particular strategy.

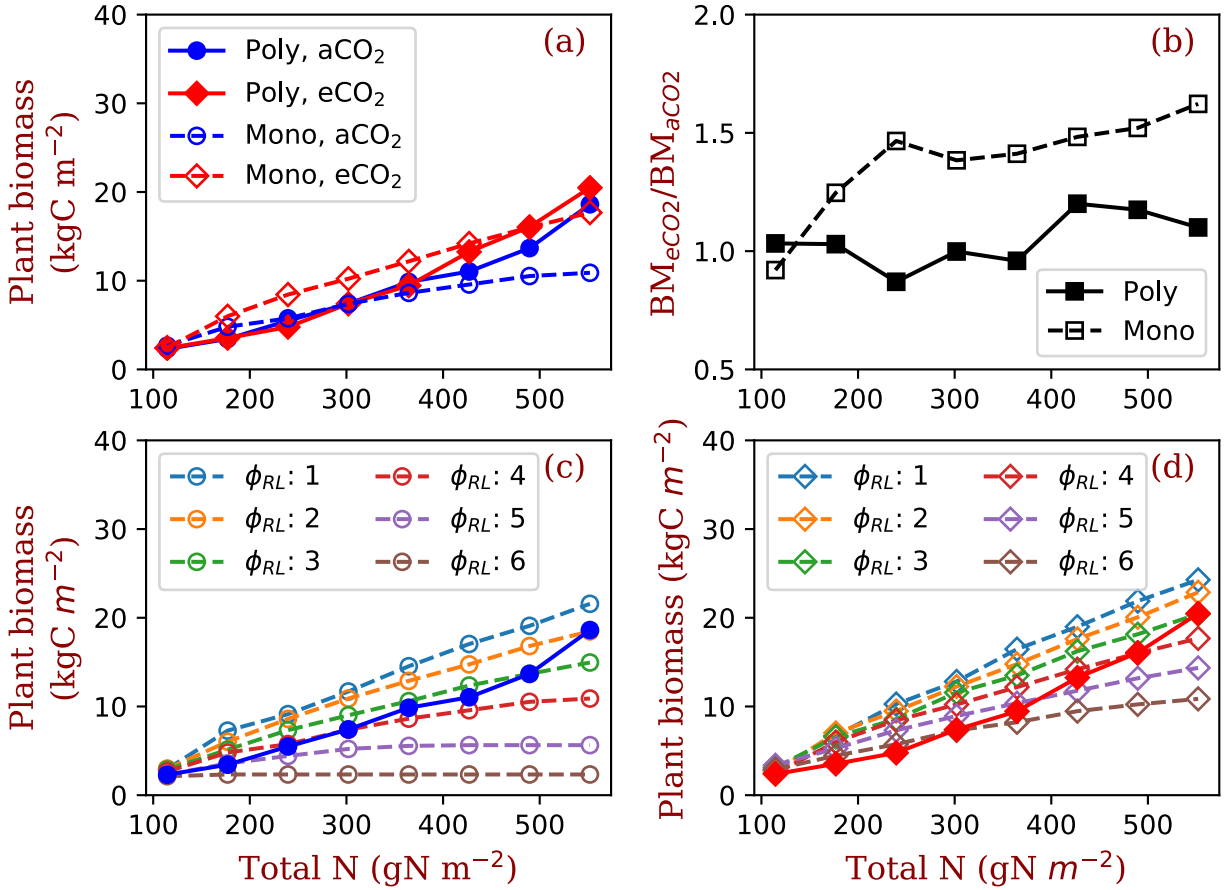
451

452 Fine root NPP does not significantly change with ecosystem total nitrogen in polyculture
453 runs, whereas it increases monotonically with increasing nitrogen in monoculture runs (Fig. 6: c).
454 Elevated [CO₂] increases fine root allocation at low nitrogen in polyculture runs but decreases
455 root allocation irrespective of nitrogen in monoculture runs (Fig. 6: c). The fraction of NPP
456 allocated to fine roots decreases with nitrogen at both CO₂ concentrations in polyculture runs but
457 it increases slightly in monoculture runs (Fig. 6: d). In monoculture runs, elevated [CO₂] reduces
458 the fraction of NPP allocated to fine roots at all nitrogen levels. In polyculture runs, fractional
459 allocation to fine roots increases at elevated [CO₂] when nitrogen is low (e.g., 114.5-302 g N m⁻²)
460 and decrease at elevated [CO₂] when nitrogen is high (e.g., 364-552 g N m⁻²).

461 In the reverse of the fine root response, NPP allocation to woody tissues increases with
462 total nitrogen in both competition and monoculture runs (Fig. 6: e). In polyculture runs, the
463 fraction of allocation to woody tissues decreases at elevated [CO₂] when ecosystem total
464 nitrogen is low (e.g., 114 – 245 g N m⁻²) and increases at elevated [CO₂] when ecosystem total
465 nitrogen is high (e.g., 302 – 552 g N m⁻²).

466 As a result of the changes in competitively-optimal ϕ_{RL} , plant biomass increases
467 dramatically with ecosystem total nitrogen in polyculture runs compared with that in
468 monoculture runs (Fig. 7: a). The effects of elevated [CO₂] on plant biomass increase with
469 nitrogen in polyculture runs but are constant overall in monoculture runs (Fig. 7: b). Compared
470 with the full spread of monoculture runs with ϕ_{RL} ranging from 1 to 6, polyculture runs have
471 high root allocation at low nitrogen and low root allocation at high nitrogen due to changes in the
472 dominant competitive allocation strategy, which amplifies plant biomass responses to elevated
473 [CO₂] with increasing nitrogen (Fig. 7: c and d).

474



475

476

Figure 7 Plant biomass responses to elevated $[\text{CO}_2]$ and nitrogen

477 Panel a shows the equilibrium plant biomass (means of simulated plant biomass from model run
 478 year 1400 to 1800) in polyculture runs and monoculture runs (only $\phi_{\text{RL}}=4$ shown as an example).

479 Panel b shows the ratio of simulated plant biomass at elevated $[\text{CO}_2]$ to ambient $[\text{CO}_2]$ for both
 480 competition and monoculture runs. Panels c and d show the comparisons with monoculture runs
 481 with ϕ_{RL} increasing from 1 to 6 at ambient (c) and elevated $[\text{CO}_2]$ (d). The closed symbols with
 482 solid line represent polyculture runs. The open symbols with dashed lines represent monoculture
 483 runs (ϕ_{RL} ranges from 1 to 6). ϕ_{RL} is the fixed ratio of fine root area to leaf area of a particular
 484 strategy. a CO_2 : 380 ppm; e CO_2 : 580 ppm.

485

486

487 **4 Discussion**

488 Our simulations show that the predicted responses of individual plants to elevated $[\text{CO}_2]$
489 can be significantly changed by explicit inclusion of competition processes. Here, the major
490 tradeoff for light- and N-limited trees is the relative allocation between stems and fine roots
491 (Dybzinski et al. 2011). Although the wood allocation (and thus carbon sequestration potential)
492 of every PFT used in this study increases under elevated $[\text{CO}_2]$ at all nitrogen levels (e.g. Fig. 6:
493 e dashed lines), only those PFTs that allocate more to fine roots (with lower carbon sequestration
494 potential) can survive competition under elevated $[\text{CO}_2]$ (Fig. 6: c solid lines). Put together,
495 explicit inclusion of competition processes reduces the expected increase in biomass (and thus
496 carbon sequestration potential) under elevated $[\text{CO}_2]$ compared with simulations that do not
497 include competition processes (Fig. 7: b).

498 Since there is a lack of direct observations or experiments to quantitatively validate the
499 long-term patterns predicted by our model, we did not calibrate it to fit observations at Harvard
500 Forest. In the following section, we analyze the model processes in detail and validate our
501 modeling approach by comparing the general patterns from observations and experiments with
502 model predictions. These comparisons also shed light on the modeling of allocation and
503 vegetation responses to elevated $[\text{CO}_2]$.

504

505 **4.1 Mechanisms of game-theoretic allocation modeling and simulation results validation**

506 In our model, the allocation of carbon and nitrogen within an individual tree is based on
507 allometric scaling (Eq. 2), functional relationships (Eq. 3), and optimization of resource usage

508 (Eq. 7). Generally, the allometric scaling relationships define the maximum leaf and fine root
509 surface area at a given tree size, and the functional relationships define the ratios of leaf area to
510 sapwood cross-sectional area and fine root surface area. These rules are commonly used in
511 ecosystem models (Franklin et al., 2012) and have been shown to generate reasonable
512 predictions (De Kauwe et al., 2014; Valentine and Mäkelä, 2012). These rules implicitly define
513 the priority of allocation to leaves and fine roots but allow for structurally-unlimited stem growth
514 when resources (carbon and nitrogen in this study) are available (i.e., the remainder goes to
515 stems after leaf and fine root growth) and NSC is not accumulated exaggeratedly when
516 ecosystem nitrogen is limited (Fig. S6).

517 We used a tuning parameter, maximum leaf and fine root allocation, $f_{LFR,max}$, to constrain
518 the maximum allocation to leaves and fine roots in order to maintain a minimum growth rate of
519 wood in years of low productivity. This is consistent with wood growth patterns in temperate
520 trees, where new wood tissues must be continuously produced (especially early in the growing
521 season) to maintain the functions of tree trunks and branches (Cuny et al., 2012; Michelot et al.,
522 2012; Plomion et al., 2001). This parameter does not change the fact that leaves and fine roots
523 are the priority in allocation, since allocation ratios to stems are around 0.4~0.7 in temperate
524 forests (Curtis et al., 2002; Litton et al., 2007). With a value of 0.85, parameter $f_{LFR,max}$ seldom
525 affects the overall carbon allocation ratios of leaves, fine roots, and stems. If $f_{LFR,max} = 1$ (i.e., the
526 highest priority for leaf and fine root growth), simulated trunk radial growth would have
527 unreasonably high interannual variation because leaf and fine root growth would use all carbon
528 to approach to their targets, leaving nothing for stems in some years of low productivity.

529 The simulation of competition for light and soil resources is based on two fundamental
530 mechanisms: 1) competition for light is based on the height of trees according to the PPA model,

531 which assumes trees have perfectly plastic crown to capture light via stem (trunk) and branch
532 phototropism (Strigul et al., 2008); and 2) individual soil N uptake is linearly dependent on the
533 fine root surface area of an individual tree relative to that of its neighbors (Dybzinski et al., 2019;
534 McMurtrie et al., 2012; Weng et al., 2017). These two mechanisms define an allocational
535 tradeoff between wood and fine roots for carbon and nitrogen investment in different CO₂
536 concentrations and nitrogen environments. Including explicit competition for these resources to
537 determine the dominant strategies results in very different predicted allocation patterns – and
538 thus ecosystem level responses – than those of strategies in the absence of competition. For
539 example, fractional wood allocation increases with increasing nitrogen availability under
540 competitive allocation but decreases – *the opposite qualitative response* – under a fixed strategy
541 (Fig. 6: f). Consequently, equilibrium plant biomass is predicted to increase much more with
542 increasing nitrogen availability under a competitive strategy (Fig. 4: c, d). In nature, the effects
543 of competition on dominant plant traits may occur through species replacement or community
544 assembly (akin to the mechanism in our model) (e.g., Douma et al., 2012), but it may also occur
545 through adaptive plastic responses or in-place sub-population evolution of ecotypes (Grams and
546 Andersen, 2007; McNickle and Dybzinski, 2013; Smith et al., 2013).

547 Generally, the predictions from competitively-optimal allocation strategies predicted by
548 our model can be found in large scale forest censuses and site-level experiments, such as: 1) high
549 nitrogen environments (i.e., productive environments) favor high wood allocation and low root
550 allocation (Litton et al., 2003; Poorter et al., 2012); 2) elevated [CO₂] increases root allocation
551 (Drake et al., 2011; Iversen, 2010; Jackson et al., 2009; Nie et al., 2013; Smith et al., 2013); 3)
552 low nitrogen availability limits vegetation biomass responses to elevated [CO₂] as a result of
553 high root allocation or root exudation (Jiang et al., 2019a; Norby and Zak, 2011); and 4)

554 increases in vegetation biomass at elevated [CO₂] are largely due to high wood allocation (Norby
555 and Zak, 2011; Walker et al., 2019). These predictions emerge from the fundamental
556 assumptions of our model without tuning parameters to fit the data, providing some confidence
557 in the robustness of our approach.

558 The literature on experimental responses of plant community to elevated [CO₂] shows
559 that the responses vary with site characteristics, forest composition, stand age, plant
560 physiological responses, and soil microbial feedbacks (Norby and Zak, 2011; Terrer et al., 2016,
561 2018). For example, in Duke Free Air CO₂ Enhancement (FACE) experiment, where the major
562 trees are loblolly pine (*Pinus taeda*), increases in root production at elevated [CO₂] stimulated
563 increased nitrogen supply that allowed the forest to sustain higher productivity (Drake et al.,
564 2011). However, in Oak Ridge FACE, where the major trees are sweetgum (*Liquidambar*
565 *styraciflua*), increased fine-root production under elevated [CO₂] did not result in increased net
566 nitrogen mineralization and increases in root production declined after eight years of CO₂
567 enhancement (Iversen, 2010; Norby and Zak, 2011). In EucFACE (Jiang et al., 2019a), where the
568 major trees are *Eucalyptus tereticornis* and the soil is infertile, trees significantly increased their
569 root exudation under limited nutrient supplies but had no significant increase in biomass in
570 response to elevated [CO₂]. The BangorFACE experiment (Smith et al., 2013) found that
571 interspecific competition (*Alnus glutinosa*, *Betula pendula* and *Fagus sylvatica*) resulted in
572 greater increases in root biomass at elevated [CO₂]. Leaf area index (LAI) responses to elevated
573 [CO₂] are also highly varied. As summarized by Norby and Zak (2011), low LAI (in this case,
574 open canopy) sites showed significant increases in LAI and high LAI (in this case, closed
575 canopy) sites showed low increases or even decreases in LAI. They concluded that LAI in

576 closed-canopy forests is not responsive to elevated [CO₂] (Norby et al., 2003; Norby and Zak,
577 2011).

578 The nature of developing a model with generic assumptions and balanced processes
579 reduces its capability to predict all of these responses. For example, plants have a variety of
580 physiological mechanisms to deal with excessive carbon supply when plant demand (i.e., “sink”)
581 is relatively low (Fatichi et al., 2019; Körner, 2006), such as down-regulating leaf photosynthesis
582 rate by the accumulated assimilates (Goldschmidt and Huber, 1992) or respiring excessive
583 carbohydrates to regenerate substrates for photosynthesis (Atkin and Macherel, 2009). But these
584 mechanisms are short-term physiological responses (minutes to hours, sometimes days) for
585 plants in situations of temporary nitrogen shortage, high irradiation, or drought stress. It is not
586 “economically” sustainable in an infertile environment to maintain highly productive leaves but
587 often suppress their photosynthesis or respire a large portion of their assimilated carbon.

588 Root exudation is a critical process for plants. It can stimulate soil organic matter
589 decomposition and nitrogen mineralization to facilitate soil nitrogen supply at the expense of
590 carbon (Cheng, 2009; Cheng et al., 2014; Drake et al., 2011; Phillips et al., 2011). The process of
591 root exudation has been adopted by many models to couple with microbial processes in the
592 determination of soil organic matter decomposition (Sulman et al., 2014; Wieder et al., 2014,
593 2015). Some carbon-only models, e.g., LM3 (Shevliakova et al., 2009), the parent model of this
594 one, and TECO (Luo et al., 2001), incorporate root exudation to put extra carbon into the soil in
595 order to avoid down-regulating canopy photosynthesis or overestimating vegetation biomass,
596 both of which had been tuned against data. However, in a demographic competition model like
597 this one, individual plants cannot reap a reward from root exudation as they do in nature when
598 the microbial activities are not fully coupled and the nitrogen in soil is assumed fully accessible

599 by roots of all individuals. Therefore, root exudation is not a competitive strategy in the system
600 defined by the assumptions of this model.

601 Since the purpose of this study is to explore long-term ecological strategies in different
602 but relatively stable environments, we did not include these processes, especially since they
603 present additional challenges in balancing the complexity of the tradeoffs between modeled
604 demographic processes and plant traits. However, the lack of these processes does limit the
605 predictions of instantaneous responses to variation in environmental conditions or resource
606 supply and possibly of some long-term vegetation characteristics as well. For example, our
607 model predicts reduced LAI under nitrogen limitation (Fig. S7) based on first principles, but it is
608 incidentally the only mechanism that reduces the whole-canopy photosynthesis rate in our
609 model. There are mechanisms that increase nitrogen use efficiency at the expense of carbon by
610 increasing LMA and therefore leaf longevity to maintain high LAI and high canopy-level
611 photosynthesis rates (Aerts, 1995, 1999; Aerts and Chapin, 1999; Givnish, 2002). We did not
612 include these mechanisms in our simulations, although they are well-developed in this model
613 (Weng et al. 2017), because we wished to focus on the strategy of allocation. The clear
614 descriptions of our model’s assumptions, its traceable processes, and inclusion of the tradeoffs
615 involved in aboveground and belowground competition provide a useful benchmark from which
616 to incorporate additional mechanisms and tradeoffs.

617

618 **4.2 Root overproliferation vs. wood allocation**

619 The allocation strategy that maximizes site vegetation biomass allocates very little to fine
620 roots (Figs. 3 and S1). In contrast, the competitively optimal strategy allocates more carbon to
621 fine roots, termed “fine-root overproliferation” in the literature (Gersani et al., 2001; McNickle

622 and Dybzinski, 2013; O'Brien et al., 2005). It is the result of a competitive “arms race”: while
623 increasing fine root area under elevated [CO₂] does not result in more nitrogen for an individual,
624 failing to do so would cede some of that individual’s nitrogen to its neighbors. Because most
625 nitrogen uptake is via mass flow and diffusion (Oyewole et al., 2017) and because both of these
626 mechanisms depend on sink strength, individuals with *relatively* greater fine root mass than their
627 neighbors take a greater share of nitrogen, as was recently demonstrated empirically (Dybzinski
628 et al., 2019; Kulmatiski et al., 2017). Thus, fine roots may overproliferate for competitive
629 reasons relative to lower optimal fine root mass in the hypothetical absence of an evolutionary
630 history of competition (Craine, 2006; McNickle and Dybzinski, 2013). This may also explain
631 why root C:N ratio is highly variable (Dybzinski et al., 2015; Luo et al., 2006; Nie et al., 2013): a
632 high density of fine roots in soil may be more important than the high absorption ability of a
633 single root in competing for soil nitrogen in the usually low mineral nitrogen soils.

634 Root overproliferation is still controversial in experiments. For example, Gersani et al.
635 (2001) and O'Brien (2005) found that competing plants generated more roots than those
636 growing in isolation; whereas McNickle and Brown (2014) found that competing plants
637 generated comparable roots to those growing in isolation. Compared to modeled roots, real roots
638 are far more adaptive and complex at modifying their growth patterns in response to soil nutrient
639 and water dynamics (Hodge, 2009). The root growth strategies in response to competition also
640 vary with species (Belter and Cahill, 2015). The mechanisms of self-recognition of inter- and
641 intra- roots also can lead to varied behavior of root growth (Chen et al., 2012). However, all of
642 the aforementioned studies considered only *plastic* root overproliferation, where individuals
643 produce more roots in the presence of other individuals than they do in isolation, analogous to
644 stem elongation of crowded seedlings (Dudley and Schmitt, 1996). A portion of root

645 overproliferation may also be *fixed*, analogous to trees that still grow tall even when grown in
646 isolation. Dybzinski et al. (2019) showed that plant community nitrogen uptake rate was
647 independent of fine root mass in seedlings of numerous species, suggesting a high degree of
648 fixed fine root overproliferation. To improve root competition models, more detailed
649 experiments that control root growth should be conducted to quantify the marginal benefits of
650 roots in isolated, monoculture, and polyculture environments.

651 At high soil nitrogen, height-structured competition for light (also a game-theoretic
652 response, Falster and Westoby, 2003; Givnish, 1982) prevails, and trees with greater *relative*
653 allocation to trunks prevail. The balance between these two competitive priorities (fine roots vs.
654 stems) can be observed in our model predictions as a shift from fine root allocation to wood
655 allocation as soil nitrogen increases. The increases in the critical height (i.e. the context-
656 dependent height of the shortest tree in canopy layer in the PPA) from low nitrogen to high
657 nitrogen indicates a shift from the importance of competition for soil nitrogen to the importance
658 of competition for light as ecosystem nitrogen increases (Fig. S8). Because the most competitive
659 type shifts from high fine root allocation to low fine root allocation as ecosystem total nitrogen
660 increases, increases in NPP and plant biomass across the nitrogen gradient are greater than the
661 increases in NPP and plant biomass assuming allocational strategies in the absence of
662 competition (Fig. 3). This greatly reduces the carbon cost of belowground competition as
663 ecosystem total nitrogen increases. The decrease in the fraction of NPP allocated to leaves at
664 elevated [CO₂] (Fig. 6: b) occurs because of increases in total NPP and nearly constant absolute
665 NPP allocation to foliage (Fig. 6: a).

666

667 **4.3 Model complexity and uncertainty**

668 Compared with the conventional pool-based vegetation models that use pools and fluxes
669 to represent plant demographic processes at a land simulation unit (e.g., grid or patch), VDMs
670 add two more layers of complexity. The first is the inclusion of stochastic birth and mortality
671 processes of individuals (i.e., demographic processes). These processes allow the models to
672 predict population dynamics and transient vegetation structure, such as size-structured
673 distribution and crown organization (e.g., Moorcroft et al., 2001; Strigul et al., 2008). With
674 changes in vegetation structure, allocation and mortality rates can change, generating a different
675 carbon storage accumulation curve compared with those predicted by pool-based models where
676 vegetation structure is not explicitly represented (e.g., Weng et al., 2015). The second is the
677 simulated shift in dominant plant traits during succession due to the shifting of competitive
678 outcomes among different PFTs, which changes the allocation between fast- and slow-turnover
679 pools and thus the parameters of allocation and the residence time of carbon in the ecosystem.

680 Together, these mechanisms may alter long-term predictions of terrestrial carbon cycle due
681 to changes in PFT-based parameters (Dybzinski et al., 2011; Farrior et al., 2013; Weng et al.,
682 2015). As described in Introduction, current pool-based models can be described by a linear
683 system of equations characterized by the key parameters of allocation, residence time, and
684 transfer coefficients (Eq. 1) with the rigid assumption of unchangeable plant types (Luo et al.,
685 2012; Xia et al., 2013). In VDMs however, allocation, residence time, leaf traits, phenology,
686 mortality, plant forms, and their responses to climate change are all strategies of competition
687 whose success varies with the environmental conditions and the traits of the individuals they are
688 competing against.

689 Many tradeoffs between plant traits can shift in response to environmental and biotic
690 changes, limiting the applicability of varying a single trait, as we have in this study. For example,

691 allocation, leaf traits, mycorrhizal types, and nitrogen fixation can all change with ecosystem
692 nitrogen availability (Menge et al., 2017; Ordoñez et al., 2009; Phillips et al., 2013; Vitousek et
693 al., 2013). The unrealistic effects of model simplification can be corrected by adding important
694 tradeoffs that are missing. For example, the positive feedback between root allocation and SOM
695 decomposition plays a role in mitigating the effects of tragedies of the commons of root over-
696 proliferation (e.g., Gersani et al., 2001; Zea-Cabrera et al., 2006) due to a negative feedback
697 induced by root turnover. High root allocation increases the decomposition rate of SOM and the
698 supply of mineral nitrogen because of the high turnover rate of root litter, which favors a strategy
699 of high wood allocation and reduces the competitive optimal fine root allocation. This negative
700 feedback indicates that the model structure is flexible and that we can incorporate correct
701 mechanisms step by step to improve model prediction skills. Testing single strategies is still a
702 necessary step to improving our understanding of the system and prediction skills of the models,
703 though it could lead to unrealistic responses sometimes.

704 We found that model predictions can differ significantly in response to seemingly-small
705 variations in basic assumptions or quantitative relationships. For example, our model predicts
706 that the ratio of plant biomass under elevated [CO₂] relative to plant biomass under ambient
707 [CO₂] should increase with increasing nitrogen due to the shift of carbon allocation from fine
708 roots to woody tissues. In contrast, the analytic model of Dybzinski *et al.* (2015) predicts that the
709 ratio of plant biomass under elevated [CO₂] relative to plant biomass under ambient [CO₂]
710 should be largely independent of total nitrogen because of an increasing shift in carbon allocation
711 from long-lived, low-nitrogen wood to short-lived, high-nitrogen fine roots under elevated [CO₂]
712 and with increasing nitrogen. This significant difference between these two predictions traces
713 back to differences in how fine root stoichiometry is handled in the two models. In the model of

714 Dybzinski *et al.* (2015), the fine root C:N ratio is flexible and the marginal nitrogen uptake
715 capacity per unit of carbon allocated to fine roots depends on its nitrogen concentration. Like the
716 model presented here, the model of Dybzinski *et al.* (2015) predicts decreasing fine root mass
717 with increasing nitrogen availability. *Unlike* the model presented here (which has constant fine
718 root nitrogen concentration), the model of Dybzinski *et al.* (2015) predicts increasing fine root
719 nitrogen concentration with increasing nitrogen availability. As a result, there is less nitrogen to
720 allocate to wood as nitrogen increases in the model of Dybzinski *et al.* (2015) than there is in the
721 model presented here. These countervailing factors even out the ratio of plant biomass under
722 elevated [CO₂] relative to plant biomass under ambient [CO₂] across the nitrogen gradient in
723 Dybzinski *et al.* (2015), whereas their absence amplifies this ratio with increasing nitrogen in the
724 model presented here. Our ability to diagnose and understand this discrepancy highlights the
725 utility of deploying closely-related analytical and simulation models (Weng *et al.*, 2017).

726 We conducted simulations only at one site for the purpose of exploring the general
727 patterns of competitively optimal allocation strategies and their responses to elevated [CO₂] at
728 different nitrogen availabilities. We can speculate about shifts in the competitively optimal
729 allocation strategy in different forest biomes by considering the effects of temperature on soil
730 nitrogen supply via the SOM's decomposition rate and its positive effect on net nitrogen
731 mineralization. For example, the SOM decomposition rate is usually high in warm regions and
732 low in cold regions (Davidson and Janssens, 2006) assuming there are no water limitations and
733 SOM is equilibrated with carbon input. According to our model, allocation to roots is high in low
734 nitrogen supply conditions (cold regions) and low in high nitrogen supply conditions (warm
735 regions). This pattern can be found from temperate to boreal forest zones (Cairns *et al.*, 1997;
736 Gower *et al.*, 2001; Reich *et al.*, 2014; Zadworny *et al.*, 2016). Temperature also alters NPP, *i.e.*,

737 carbon supply: as temperature goes down, NPP decreases and nitrogen demand decreases,
738 alleviating nitrogen limitation and leading to shifts of allocation to stems. So, the differences in
739 temperature effects on photosynthesis and SOM decomposition will determine competitive
740 allocation strategy. Since SOM decomposition is more sensitive to temperature than gross
741 primary production is at long-temporal and large-spatial scales (Beer et al., 2010; Carey et al.,
742 2016; Crowther et al., 2016), our model suggests that allocation will shift to wood in a warming
743 world. Whether the carbon stored in that wood is enough to offset the carbon released from
744 increasing soil respiration is a critical question.

745 Water is also a critical factor affecting allocation and its responses to elevated [CO₂].
746 Low soil moisture usually leads to high allocation to roots (Poorter et al., 2012). Elevated CO₂
747 can reduce transpiration (as found in our study as well, Figs. S9~S11) and therefore increase soil
748 moisture, resulting in increases in allocation to stems and aboveground biomass (Walker et al.,
749 2019). A game-theoretic modeling study using the PPA framework shows that the competitively
750 optimal allocation strategy shifts to high wood allocation at elevated [CO₂] in environments with
751 water limitation (Farrior et al., 2015). This is opposite to the elevated [CO₂] effects on allocation
752 in nitrogen-limited environments as simulated in this study. According to field experiments, fine
753 root allocation is more responsive to nitrogen changes than it to soil moisture changes (Canham
754 et al., 1996; Poorter et al., 2012). Poorter et al. (2012) attribute the mechanisms to the optimal
755 strategies in response to the relative stable nitrogen supply and stochastic water input in soil. The
756 vertical distribution of roots and the contributions of roots in different layers to water and
757 nitrogen uptake also suggest that the uptake of soil nutrients are dominant in shaping root system
758 architecture (Chapman et al., 2012; Morris et al., 2017), though root growth and turnover are

759 flexible and sensitive to nitrogen and water supply (Deak and Malamy, 2005; Linkohr et al.,
760 2002; Pregitzer et al., 1993).

761

762 **4.4 Common principles for allocation modeling and implications**

763 As shown in model inter-comparison studies, the mechanisms of modeling allocation
764 differ very much, leading to high variation in their predictions (e.g., De Kauwe et al. 2014).
765 Calibrating model parameters to fit data may not increase model predictive skill because data are
766 often also highly variable. Franklin et al. (20`12) suggest that in order to build realistic and
767 predictive allocation models, we should correctly identify and implement fundamental principles.
768 Our model predicts similar patterns to those predicted by the model of Valentine and Mäkelä
769 (2012), which has very different processes of plant growth and allocation. However, these two
770 models share fundamental principles, including 1) evolutionary- or competitive-optimization, 2)
771 capped leaves and fine roots at given tree sizes, 3) structurally unlimited stem allocation (i.e.,
772 optimizing carbon use) because the woody tissues can serve as unlimited sink for surplus carbon,
773 and 4) height-structure competition for light and root-mass-based competition for soil resources.
774 The principles 2 and 3 are commonly used in models (De Kauwe et al., 2014; Jiang et al.,
775 2019b). However, the different rules of implementing them (e.g., allometric equation, functional
776 relationships, etc.) lead to highly varied predictions (as shown in De Kauwe et al., 2014), though
777 model formulations may be very similar.

778 In competitively-optimal models, such as this study and also Valentine and Mäkelä (2012),
779 the competition processes generate similar emergent patterns by selecting those that can survive
780 in competition, regardless the details of those differences. The competition processes also make
781 the details of allocation settings for a single PFT and their direct responses to elevated [CO₂] less

782 important, because competition processes will select out the most competitive strategy from
783 diverse strategies in response to changes in [CO₂] and nitrogen. Our study and Valentine and
784 Mäkelä (2012), posit a fundamental tradeoff between light competition and nitrogen competition
785 via allocation based on insights gained from simpler models (e.g., Dybzinski et al., 2015; Mäkelä
786 et al., 2008) for predicting allocation as an emergent property of competition. One advantage of
787 building a model in this way is that the vegetation dynamics are predicted from first principles,
788 rather than based on the correlations between vegetation properties and environmental
789 conditions. With these first principles, the models can produce reasonable predictions, though the
790 details of physiological and demographic processes vary among models.

791 For vegetation models designed to predict the effects of climate change, the important
792 operational distinction is that the fundamental rules cannot or will not change as climate changes.
793 Nor, presumably, will the underlying ecological and evolutionary processes change as climate
794 changes. The emergent properties can change as climate changes however, and the models built
795 on the “scale-appropriate” unbreakable constraints and ecological and evolutionary processes
796 will be able to accurately predict changes in emergent ecosystem properties (Weng et al., 2017).
797 In our opinion, the scientific effort to build better models is better served by understanding
798 unrealistic predictions than by “fixing” them with unreliable mechanisms when there is a lack of
799 data or theory to make them consistent with observations. Validating assumptions and initial
800 responses are critical, and the long-term responses can be validated via spatial patterns.

801 This modeling approach also demands improvement in model validation and benchmarking
802 systems (Collier et al., 2018; Hoffman et al., 2017). As shown in this study, allocation responses
803 to elevated CO₂ at different nitrogen levels in monoculture runs are opposite to those in
804 competitive-allocation runs. For example, in monoculture runs, elevated [CO₂] increases wood

805 allocation and decreases fine root allocation at low nitrogen; whereas in competitive-allocation
806 runs elevated [CO₂] leads to low wood allocation and high fine root allocation. Simply
807 calibrating our model against short-term observational data may improve the agreement with
808 observations but would not change the model's predictions because the model's predictions
809 emerge from its fundamental assumptions.

810

811 **5 Conclusions**

812 Our study illustrates that including the competition processes for light and soil resources in
813 a game-theoretic vegetation demographic model can substantially change the prediction of the
814 contribution of ecosystems to the global carbon cycle. Allowing the model to explicitly track the
815 competitive allocation strategies can generate significantly different ecosystem-level predictions
816 (e.g., biomass and ecosystem carbon storage) than those of strategies in the absence of explicit
817 competition. Building such a model requires differentiating between the unbreakable tradeoffs of
818 plant traits and ecological processes from the emergent properties of ecosystems. Drawing on
819 insights from closely-related analytical models to develop and understand more complicated
820 simulation models seems, to us, indispensable. Evaluating these models also requires an updated
821 model benchmarking system that includes the metrics of competitive plant traits during the
822 development of ecosystems and their responses to global change factors.

823

824 **Acknowledgements**

825 This work was supported by NASA Modeling, Analysis, and Prediction (MAP) Program
826 (NNH16ZDA001N-MAP), USDA Forest Service Northern Research Station (Agreement 13-JV-

827 11242315-066), and the Carbon Mitigation Initiative at Princeton University. C.E.F

828 acknowledges support from the University of Texas at Austin.

829

830 **Codes and data availability**

831 The model codes used in this study, simulated data, and Python scripts used in this study are in

832 Github (<https://github.com/wengensheng/BiomeE-Allocation>).

833

834 **Reference**

- 835 Aber, J. D., Magill, A., Boone, R., Melillo, J. M. and Steudler, P.: Plant and Soil Responses to
836 Chronic Nitrogen Additions at the Harvard Forest, Massachusetts, *Ecological Applications*, 3(1),
837 156–166, doi:10.2307/1941798, 1993.
- 838 Aerts, R.: The advantages of being evergreen, *Trends in ecology & evolution*, 10(10), 402–407,
839 doi:10.1016/S0169-5347(00)89156-9, 1995.
- 840 Aerts, R.: Interspecific competition in natural plant communities: mechanisms, trade-offs and
841 plant-soil feedbacks, *Journal of Experimental Botany*, 50(330), 29–37,
842 doi:10.1093/jxb/50.330.29, 1999.
- 843 Aerts, R. and Chapin, F. S.: The Mineral Nutrition of Wild Plants Revisited: A Re-evaluation of
844 Processes and Patterns, in *Advances in Ecological Research*, vol. 30, edited by A. H. Fitter and D.
845 G. Raffaelli, pp. 1–67, Academic Press., 1999.
- 846 Arora, V. K. and Boer, G. J.: A parameterization of leaf phenology for the terrestrial ecosystem
847 component of climate models, *Global Change Biology*, 11(1), 39–59, doi:10.1111/j.1365-
848 2486.2004.00890.x, 2005.
- 849 Atkin, O. K. and Macherel, D.: The crucial role of plant mitochondria in orchestrating drought
850 tolerance, *Ann Bot*, 103(4), 581–597, doi:10.1093/aob/mcn094, 2009.
- 851 Barr, A. G., Ricciu, D. M., Schaefer, K., Richardson, A., Agarwal, D., Thornton, P. E., Davis, K.,
852 Jackson, B., Cook, R. B., Hollinger, D. Y., Van Ingen, C., Amiro, B., Andrews, A., Arain, M. A.,
853 Baldocchi, D., Black, T. A., Bolstad, P., Curtis, P., Desai, A., Dragoni, D., Flanagan, L., Gu, L., Katul,
854 G., Law, B. E., Lafleur, P. M., Margolis, H., Matamala, R., Meyers, T., McCaughey, J. H., Monson,
855 R., Munger, J. W., Oechel, W., Oren, R., Roulet, N. T., Torn, M. and Verma, S. B.: NACP Site:
856 Tower Meteorology, Flux Observations with Uncertainty, and Ancillary Data, ,
857 doi:10.3334/ornl/daac/1178, 2013.
- 858 Beer, C., Reichstein, M., Tomelleri, E., Ciais, P., Jung, M., Carvalhais, N., Rodenbeck, C., Arain, M.
859 A., Baldocchi, D., Bonan, G. B., Bondeau, A., Cescatti, A., Lasslop, G., Lindroth, A., Lomas, M.,
860 Luyssaert, S., Margolis, H., Oleson, K. W., Rouspard, O., Veenendaal, E., Viovy, N., Williams, C.,
861 Woodward, F. I. and Papale, D.: Terrestrial Gross Carbon Dioxide Uptake: Global Distribution
862 and Covariation with Climate, *Science*, 329(5993), 834–838, doi:10.1126/science.1184984,
863 2010.
- 864 Belter, P. R. and Cahill, J. F.: Disentangling root system responses to neighbours: identification
865 of novel root behavioural strategies, *AoB PLANTS*, 7, plv059, doi:10.1093/aobpla/plv059, 2015.
- 866 Bloom, A. A., Exbrayat, J.-F., van der Velde, I. R., Feng, L. and Williams, M.: The decadal state of
867 the terrestrial carbon cycle: Global retrievals of terrestrial carbon allocation, pools, and
868 residence times, *Proceedings of the National Academy of Sciences*, 113(5), 1285–1290,
869 doi:10.1073/pnas.1515160113, 2016.

870 Cairns, M. A., Brown, S., Helmer, E. H. and Baumgardner, G. A.: Root biomass allocation in the
871 world's upland forests, *Oecologia*, 111(1), 1–11, doi:10.1007/s004420050201, 1997.

872 Canham, C. D., Berkowitz, A. R., Kelly, V. R., Lovett, G. M., Ollinger, S. V. and Schnurr, J.: Biomass
873 allocation and multiple resource limitation in tree seedlings, *Canadian Journal of Forest
874 Research-Revue Canadienne De Recherche Forestiere*, 26(9), 1521–1530, doi:10.1139/x26-171,
875 1996.

876 Cannell, M. G. R. and Dewar, R. C.: Carbon Allocation in Trees: a Review of Concepts for
877 Modelling, in *Advances in Ecological Research*, vol. 25, pp. 59–104, Elsevier., 1994.

878 Carey, J. C., Tang, J., Templer, P. H., Kroeger, K. D., Crowther, T. W., Burton, A. J., Dukes, J. S.,
879 Emmett, B., Frey, S. D., Heskell, M. A., Jiang, L., Machmuller, M. B., Mohan, J., Panetta, A. M.,
880 Reich, P. B., Reinsch, S., Wang, X., Allison, S. D., Bamminger, C., Bridgham, S., Collins, S. L., de
881 Dato, G., Eddy, W. C., Enquist, B. J., Estiarte, M., Harte, J., Henderson, A., Johnson, B. R., Larsen,
882 K. S., Luo, Y., Marhan, S., Melillo, J. M., Peñuelas, J., Pfeifer-Meister, L., Poll, C., Rastetter, E.,
883 Reinmann, A. B., Reynolds, L. L., Schmidt, I. K., Shaver, G. R., Strong, A. L., Suseela, V. and
884 Tietema, A.: Temperature response of soil respiration largely unaltered with experimental
885 warming, *Proceedings of the National Academy of Sciences*, 113(48), 13797–13802,
886 doi:10.1073/pnas.1605365113, 2016.

887 Chapman, N., Miller, A. J., Lindsey, K. and Whalley, W. R.: Roots, water, and nutrient
888 acquisition: let's get physical, *Trends in Plant Science*, 17(12), 701–710,
889 doi:10.1016/j.tplants.2012.08.001, 2012.

890 Chen, B. J. W., Daring, H. J. and Anten, N. P. R.: Detect thy neighbor: Identity recognition at the
891 root level in plants, *Plant Science*, 195, 157–167, doi:10.1016/j.plantsci.2012.07.006, 2012.

892 Cheng, W.: Rhizosphere priming effect: Its functional relationships with microbial turnover,
893 evapotranspiration, and C-N budgets, *Soil Biology & Biochemistry*, 41(9), 1795–1801,
894 doi:10.1016/j.soilbio.2008.04.018, 2009.

895 Cheng, W., Parton, W. J., Gonzalez-Meler, M. A., Phillips, R., Asao, S., McNickle, G. G., Brzostek,
896 E. and Jastrow, J. D.: Synthesis and modeling perspectives of rhizosphere priming, *New
897 Phytologist*, 201(1), 31–44, doi:10.1111/nph.12440, 2014.

898 Collier, N., Hoffman, F. M., Lawrence, D. M., Keppel-Aleks, G., Koven, C. D., Riley, W. J., Mu, M.
899 and Randerson, J. T.: The International Land Model Benchmarking (ILAMB) System: Design,
900 Theory, and Implementation, *Journal of Advances in Modeling Earth Systems*, 10(11), 2731–
901 2754, doi:10.1029/2018MS001354, 2018.

902 Compton, J. E. and Boone, R. D.: Long-Term Impacts of Agriculture on Soil Carbon and Nitrogen
903 in New England Forests, *Ecology*, 81(8), 2314, doi:10.2307/177117, 2000.

904 Craine, J. M.: Competition for Nutrients and Optimal Root Allocation, *Plant and Soil*, 285(1–2),
905 171–185, doi:10.1007/s11104-006-9002-x, 2006.

906 Crowther, T. W., Todd-Brown, K. E. O., Rowe, C. W., Wieder, W. R., Carey, J. C., Machmuller, M.
907 B., Snoek, B. L., Fang, S., Zhou, G., Allison, S. D., Blair, J. M., Bridgham, S. D., Burton, A. J.,
908 Carrillo, Y., Reich, P. B., Clark, J. S., Classen, A. T., Dijkstra, F. A., Elberling, B., Emmett, B. A.,
909 Estiarte, M., Frey, S. D., Guo, J., Harte, J., Jiang, L., Johnson, B. R., Kröel-Dulay, G., Larsen, K. S.,
910 Laudon, H., Lavallee, J. M., Luo, Y., Lupascu, M., Ma, L. N., Marhan, S., Michelsen, A., Mohan, J.,
911 Niu, S., Pendall, E., Peñuelas, J., Pfeifer-Meister, L., Poll, C., Reinsch, S., Reynolds, L. L., Schmidt,
912 I. K., Sistla, S., Sokol, N. W., Templer, P. H., Treseder, K. K., Welker, J. M. and Bradford, M. A.:
913 Quantifying global soil carbon losses in response to warming, *Nature*, 540(7631), 104–108,
914 doi:10.1038/nature20150, 2016.

915 Cuny, H. E., Rathgeber, C. B. K., Lebourgeois, F., Fortin, M. and Fournier, M.: Life strategies in
916 intra-annual dynamics of wood formation: example of three conifer species in a temperate
917 forest in north-east France, *Tree Physiology*, 32(5), 612–625, doi:10.1093/treephys/tps039,
918 2012.

919 Curtis, P. S., Hanson, P. J., Bolstad, P., Barford, C., Randolph, J. C., Schmid, H. P. and Wilson, K.
920 B.: Biometric and eddy-covariance based estimates of annual carbon storage in five eastern
921 North American deciduous forests, *Agricultural and Forest Meteorology*, 113(1–4), 3–19,
922 doi:10.1016/S0168-1923(02)00099-0, 2002.

923 Davidson, E. A. and Janssens, I. A.: Temperature sensitivity of soil carbon decomposition and
924 feedbacks to climate change, *Nature*, 440(7081), 165–173, doi:10.1038/nature04514, 2006.

925 De Kauwe, M. G., Medlyn, B. E., Zaehle, S., Walker, A. P., Dietze, M. C., Wang, Y.-P., Luo, Y., Jain,
926 A. K., El-Masri, B., Hickler, T., Wårlind, D., Weng, E., Parton, W. J., Thornton, P. E., Wang, S.,
927 Prentice, I. C., Asao, S., Smith, B., McCarthy, H. R., Iversen, C. M., Hanson, P. J., Warren, J. M.,
928 Oren, R. and Norby, R. J.: Where does the carbon go? A model-data intercomparison of
929 vegetation carbon allocation and turnover processes at two temperate forest free-air CO₂
930 enrichment sites, *New Phytologist*, 203(3), 883–899, doi:10.1111/nph.12847, 2014.

931 Deak, K. I. and Malamy, J.: Osmotic regulation of root system architecture, *The Plant Journal*,
932 43(1), 17–28, doi:10.1111/j.1365-313X.2005.02425.x, 2005.

933 DeAngelis, D. L., Ju, S., Liu, R., Bryant, J. P. and Gourley, S. A.: Plant allocation of carbon to
934 defense as a function of herbivory, light and nutrient availability, *Theoretical Ecology*, 5(3), 445–
935 456, doi:10.1007/s12080-011-0135-z, 2012.

936 Douma, J. C., de Haan, M. W. A., Aerts, R., Witte, J.-P. M. and van Bodegom, P. M.: Succession-
937 induced trait shifts across a wide range of NW European ecosystems are driven by light and
938 modulated by initial abiotic conditions: Trait shifts during succession, *Journal of Ecology*, 100(2),
939 366–380, doi:10.1111/j.1365-2745.2011.01932.x, 2012.

940 Drake, J. E., Gallet-Budynek, A., Hofmockel, K. S., Bernhardt, E. S., Billings, S. A., Jackson, R. B.,
941 Johnsen, K. S., Lichter, J., McCarthy, H. R., McCormack, M. L., Moore, D. J. P., Oren, R.,
942 Palmroth, S., Phillips, R. P., Pippen, J. S., Pritchard, S. G., Treseder, K. K., Schlesinger, W. H.,

- 943 DeLucia, E. H. and Finzi, A. C.: Increases in the flux of carbon belowground stimulate nitrogen
944 uptake and sustain the long-term enhancement of forest productivity under elevated CO₂,
945 *ECOLOGY LETTERS*, 14(4), 349–357, doi:10.1111/j.1461-0248.2011.01593.x, 2011.
- 946 Dudley, S. A. and Schmitt, J.: Testing the adaptive plasticity hypothesis: density-dependent
947 selection on manipulated stem length in *Impatiens capensis*, *The American Naturalist*, 147(3),
948 445–465, doi:10.1086/285860, 1996.
- 949 Dybzinski, R., Farris, C., Wolf, A., Reich, P. B. and Pacala, S. W.: Evolutionarily Stable Strategy
950 Carbon Allocation to Foliage, Wood, and Fine Roots in Trees Competing for Light and Nitrogen:
951 An Analytically Tractable, Individual-Based Model and Quantitative Comparisons to Data,
952 *American Naturalist*, 177(2), 153–166, doi:10.1086/657992, 2011.
- 953 Dybzinski, R., Farris, C. E. and Pacala, S. W.: Increased forest carbon storage with increased
954 atmospheric CO₂ despite nitrogen limitation: a game-theoretic allocation model for trees in
955 competition for nitrogen and light, *Global Change Biology*, 21(3), 1182–1196,
956 doi:10.1111/gcb.12783, 2015.
- 957 Dybzinski, R., Kelvakis, A., McCabe, J., Panock, S., Anuchitlertchon, K., Vasarhelyi, L., Luke
958 McCormack, M., McNickle, G. G., Poorter, H., Trinder, C. and Farris, C. E.: How are nitrogen
959 availability, fine-root mass, and nitrogen uptake related empirically? Implications for models
960 and theory, *Global Change Biology*, doi:10.1111/gcb.14541, 2019.
- 961 Emanuel, W. R. and Killough, G. G.: Modeling terrestrial ecosystems in the global carbon cycle
962 with Shifts in carbon storage capacity by land-use change, *Ecology*, 65(3), 970–983,
963 doi:10.2307/1938069, 1984.
- 964 Eriksson, E.: Compartment Models and Reservoir Theory, *Annual Review of Ecology and*
965 *Systematics*, 2(1), 67–84, doi:10.1146/annurev.es.02.110171.000435, 1971.
- 966 Falster, D. and Westoby, M.: Plant height and evolutionary games, *TRENDS IN ECOLOGY &*
967 *EVOLUTION*, 18(7), 337–343, doi:10.1016/S0169-5347(03)00061-2, 2003.
- 968 Farris, C. E., Dybzinski, R., Levin, S. A. and Pacala, S. W.: Competition for Water and Light in
969 Closed-Canopy Forests: A Tractable Model of Carbon Allocation with Implications for Carbon
970 Sinks, *American Naturalist*, 181(3), 314–330, doi:10.1086/669153, 2013.
- 971 Farris, C. E., Rodriguez-Iturbe, I., Dybzinski, R., Levin, S. A. and Pacala, S. W.: Decreased water
972 limitation under elevated CO₂ amplifies potential for forest carbon sinks, *Proceedings of the*
973 *National Academy of Sciences of the United States of America*, 112(23), 7213–7218,
974 doi:10.1073/pnas.1506262112, 2015.
- 975 Fatichi, S., Pappas, C., Zscheischler, J. and Leuzinger, S.: Modelling carbon sources and sinks in
976 terrestrial vegetation, *New Phytologist*, 221(2), 652–668, doi:10.1111/nph.15451, 2019.

- 977 Fisher, R. A., Koven, C. D., Anderegg, W. R. L., Christoffersen, B. O., Dietze, M. C., Farrior, C. E.,
 978 Holm, J. A., Hurtt, G. C., Knox, R. G., Lawrence, P. J., Lichstein, J. W., Longo, M., Matheny, A. M.,
 979 Medvigy, D., Muller-Landau, H. C., Powell, T. L., Serbin, S. P., Sato, H., Shuman, J. K., Smith, B.,
 980 Trugman, A. T., Viskari, T., Verbeeck, H., Weng, E., Xu, C., Xu, X., Zhang, T. and Moorcroft, P. R.:
 981 Vegetation demographics in Earth System Models: A review of progress and priorities, *Global*
 982 *Change Biology*, 24(1), 35–54, doi:10.1111/gcb.13910, 2018.
- 983 Franklin, O., Johansson, J., Dewar, R. C., Dieckmann, U., McMurtrie, R. E., Brannstrom, A. and
 984 Dybzinski, R.: Modeling carbon allocation in trees: a search for principles, *Tree Physiology*,
 985 32(6), 648–666, doi:10.1093/treephys/tpz138, 2012.
- 986 Friend, A. D., Arneeth, A., Kiang, N. Y., Lomas, M., Ogee, J., Roedenbeckk, C., Running, S. W.,
 987 Santaren, J.-D., Sitch, S., Viovy, N., Woodward, F. I. and Zaehle, S.: FLUXNET and modelling the
 988 global carbon cycle, *Global Change Biology*, 13(3), 610–633, doi:10.1111/j.1365-
 989 2486.2006.01223.x, 2007.
- 990 Gersani, M., Brown, J. s., O'Brien, E. E., Maina, G. M. and Abramsky, Z.: Tragedy of the
 991 commons as a result of root competition, *Journal of Ecology*, 89(4), 660–669,
 992 doi:10.1046/j.0022-0477.2001.00609.x, 2001.
- 993 Givnish, T.: Adaptive significance of evergreen vs. deciduous leaves: solving the triple paradox,
 994 *Silva Fenn.*, 36(3), doi:10.14214/sf.535, 2002.
- 995 Givnish, T. J.: On the Adaptive Significance of Leaf Height in Forest Herbs, *The American*
 996 *Naturalist*, 120(3), 353–381, doi:10.1086/283995, 1982.
- 997 Goldschmidt, E. E. and Huber, S. C.: Regulation of Photosynthesis by End-Product Accumulation
 998 in Leaves of Plants Storing Starch, Sucrose, and Hexose Sugars, *Plant Physiology*, 99(4), 1443–
 999 1448, doi:10.1104/pp.99.4.1443, 1992.
- 1000 Gower, S. T., Krankina, O., Olson, R. J., Apps, M., Linder, S. and Wang, C.: Net Primary
 1001 Production and Carbon Allocation Patterns of Boreal Forest Ecosystems, *Ecological Applications*,
 1002 11(5), 1395–1411, doi:10.1890/1051-0761(2001)011[1395:NPPACA]2.0.CO;2, 2001.
- 1003 Grams, T. E. E. and Andersen, C. P.: Competition for Resources in Trees: Physiological Versus
 1004 Morphological Plasticity, in *Progress in Botany*, edited by K. Esser, U. Löttge, W. Beyschlag, and
 1005 J. Murata, pp. 356–381, Springer Berlin Heidelberg, Berlin, Heidelberg., 2007.
- 1006 Haverd, V., Smith, B., Raupach, M., Briggs, P., Nieradzick, L., Beringer, J., Hutley, L., Trudinger, C.
 1007 M. and Cleverly, J.: Coupling carbon allocation with leaf and root phenology predicts tree–grass
 1008 partitioning along a savanna rainfall gradient, *Biogeosciences*, 13(3), 761–779, doi:10.5194/bg-
 1009 13-761-2016, 2016.
- 1010 Hibbs, D. E.: Forty Years of Forest Succession in Central New England, *Ecology*, 64(6), 1394–
 1011 1401, doi:10.2307/1937493, 1983.

- 1012 Hodge, A.: Root decisions, *Plant, Cell & Environment*, 32(6), 628–640, doi:10.1111/j.1365-
1013 3040.2008.01891.x, 2009.
- 1014 Hoffman, F. M., Koven, C. D., Keppel-Aleks, G., Lawrence, D. M., Riley, W. J., Randerson, J. T.,
1015 Ahlström, A., Abramowitz, G., Baldocchi, D. D., Best, M. J., Bond-Lamberty, B., De Kauwe, M. G.,
1016 Denning, A. S., Desai, A. R., Eyring, V., Fisher, J. B., Fisher, R. A., Gleckler, P. J., Huang, M.,
1017 Hugelius, G., Jain, A. K., Kiang, N. Y., Kim, H., Koster, R. D., Kumar, S. V., Li, H., Luo, Y., Mao, J.,
1018 McDowell, N. G., Mishra, U., Moorcroft, P. R., Pau, G. S. H., Ricciuto, D. M., Schaefer, K.,
1019 Schwalm, C. R., Serbin, S. P., Shevliakova, E., Slater, A. G., Tang, J., Williams, M., Xia, J., Xu, C.,
1020 Joseph, R. and Koch, D.: 2016 International Land Model Benchmarking (ILAMB) Workshop
1021 Report., 2017.
- 1022 Iversen, C. M.: Digging deeper: fine-root responses to rising atmospheric CO₂ concentration in
1023 forested ecosystems, *New Phytologist*, 186(2), 346–357, doi:10.1111/j.1469-
1024 8137.2009.03122.x, 2010.
- 1025 Jackson, R. B., Cook, C. W., Phippen, J. S. and Palmer, S. M.: Increased belowground biomass and
1026 soil CO₂ fluxes after a decade of carbon dioxide enrichment in a warm-temperate forest,
1027 *Ecology*, 90(12), 3352–3366, doi:10.1890/08-1609.1, 2009.
- 1028 Jenkins, J. C., Chojnacky, D. C., Heath, L. S. and Birdsey, R. A.: National-Scale Biomass Estimators
1029 for United States Tree Species, *Forest Science*, 49(1), 12–35, doi:10.1093/forestscience/49.1.12,
1030 2003.
- 1031 Jiang, M., Medlyn, B. E., Drake, J. E., Duursma, R. A., Anderson, I. C., Barton, C. V. M., Boer, M.
1032 M., Carrillo, Y., Castañeda-Gómez, L., Collins, L., Crous, K. Y., De Kauwe, M. G., Emmerson, K. M.,
1033 Facey, S. L., Gherlenda, A. N., Gimeno, T. E., Hasegawa, S., Johnson, S. N., Macdonald, C. A.,
1034 Mahmud, K., Moore, B. D., Nazaries, L., Nielsen, U. N., Noh, N. J., Ochoa-Hueso, R., Pathare, V.
1035 S., Pendall, E., Pineiro, J., Powell, J. R., Power, S. A., Reich, P. B., Renchon, A. A., Riegler, M.,
1036 Rymer, P., Salomón, R. L., Singh, B. K., Smith, B., Tjoelker, M. G., Walker, J. K. M., Wujeska-
1037 Klause, A., Yang, J., Zaehle, S. and Ellsworth, D. S.: The fate of carbon in a mature forest under
1038 carbon dioxide enrichment, *BioRxiv.*, 2019a.
- 1039 Jiang, M., Zaehle, S., De Kauwe, M. G., Walker, A. P., Caldararu, S., Ellsworth, D. S. and Medlyn,
1040 B. E.: The quasi-equilibrium framework revisited: analyzing long-term CO₂ enrichment
1041 responses in plant–soil models, *Geosci. Model Dev.*, 12(5), 2069–2089, doi:10.5194/gmd-12-
1042 2069-2019, 2019b.
- 1043 Keenan, T. F., Davidson, E. A., Munger, J. W. and Richardson, A. D.: Rate my data: quantifying
1044 the value of ecological data for the development of models of the terrestrial carbon cycle,
1045 *Ecological Applications*, 23(1), 273–286, doi:10.1890/12-0747.1, 2013.
- 1046 Körner, C.: Plant CO₂ responses: an issue of definition, time and resource supply, *New Phytol.*,
1047 172(3), 393–411, doi:10.1111/j.1469-8137.2006.01886.x, 2006.

- 1048 Koven, C. D., Chambers, J. Q., Georgiou, K., Knox, R., Negron-Juarez, R., Riley, W. J., Arora, V. K.,
1049 Brovkin, V., Friedlingstein, P. and Jones, C. D.: Controls on terrestrial carbon feedbacks by
1050 productivity versus turnover in the CMIP5 Earth System Models, *Biogeosciences*, 12(17), 5211–
1051 5228, doi:10.5194/bg-12-5211-2015, 2015.
- 1052 Krinner, G., Viovy, N., de Noblet-Ducoudré, N., Ogée, J., Polcher, J., Friedlingstein, P., Ciais, P.,
1053 Sitch, S. and Prentice, I. C.: A dynamic global vegetation model for studies of the coupled
1054 atmosphere-biosphere system, *Global Biogeochemical Cycles*, 19(1),
1055 doi:10.1029/2003GB002199, 2005.
- 1056 Kulmatiski, A., Adler, P. B., Stark, J. M. and Tredennick, A. T.: Water and nitrogen uptake are
1057 better associated with resource availability than root biomass, *Ecosphere*, 8(3), e01738,
1058 doi:10.1002/ecs2.1738, 2017.
- 1059 Lacointe, A.: Carbon allocation among tree organs: A review of basic processes and
1060 representation in functional-structural tree models, *Annals of Forest Science*, 57(5), 521–533,
1061 doi:10.1051/forest:2000139, 2000.
- 1062 Leuning, R., Kelliher, F. M., Pury, D. G. G. and Schulze, E.-D.: Leaf nitrogen, photosynthesis,
1063 conductance and transpiration: scaling from leaves to canopies, *Plant Cell Environ*, 18(10),
1064 1183–1200, doi:10.1111/j.1365-3040.1995.tb00628.x, 1995.
- 1065 Linkohr, B. I., Williamson, L. C., Fitter, A. H. and Leyser, H. M. O.: Nitrate and phosphate
1066 availability and distribution have different effects on root system architecture of *Arabidopsis*,
1067 *The Plant Journal*, 29(6), 751–760, doi:10.1046/j.1365-313X.2002.01251.x, 2002.
- 1068 Litton, C., Ryan, M., Knight, D. and Stahl, P.: Soil-surface carbon dioxide efflux and microbial
1069 biomass in relation to tree density 13 years after a stand replacing fire in a lodgepole pine
1070 ecosystem, *GLOBAL CHANGE BIOLOGY*, 9(5), 680–696, doi:10.1046/j.1365-2486.2003.00626.x,
1071 2003.
- 1072 Litton, C. M., Raich, J. W. and Ryan, M. G.: Carbon allocation in forest ecosystems, *Global
1073 Change Biol*, 13(10), 2089–2109, doi:10.1111/j.1365-2486.2007.01420.x, 2007.
- 1074 Luo, Y. and Weng, E.: Dynamic disequilibrium of the terrestrial carbon cycle under global
1075 change, *Trends in Ecology & Evolution*, 26(2), 96–104, doi:10.1016/j.tree.2010.11.003, 2011.
- 1076 Luo, Y., Hui, D. and Zhang, D.: Elevated CO₂ stimulates net accumulations of carbon and
1077 nitrogen in land ecosystems: a meta-analysis, *Ecology*, 87(1), 53–63, 2006.
- 1078 Luo, Y. Q., Wu, L. H., Andrews, J. A., White, L., Matamala, R., Schafer, K. V. R. and Schlesinger,
1079 W. H.: Elevated CO₂ differentiates ecosystem carbon processes: Deconvolution analysis of Duke
1080 Forest FACE data, *Ecological Monographs*, 71(3), 357–376, doi:10.1890/0012-
1081 9615(2001)071[0357:ECDECP]2.0.CO;2, 2001.

- 1082 Luo, Y. Q., Randerson, J. T., Abramowitz, G., Bacour, C., Blyth, E., Carvalhais, N., Ciais, P.,
 1083 Dalmonech, D., Fisher, J. B., Fisher, R., Friedlingstein, P., Hibbard, K., Hoffman, F., Huntzinger,
 1084 D., Jones, C. D., Koven, C., Lawrence, D., Li, D. J., Mahecha, M., Niu, S. L., Norby, R., Piao, S. L.,
 1085 Qi, X., Peylin, P., Prentice, I. C., Riley, W., Reichstein, M., Schwalm, C., Wang, Y. P., Xia, J. Y.,
 1086 Zaehle, S. and Zhou, X. H.: A framework for benchmarking land models, *Biogeosciences*, 9(10),
 1087 3857–3874, doi:10.5194/bg-9-3857-2012, 2012.
- 1088 Magill, A. H., Aber, J. D., Currie, W. S., Nadelhoffer, K. J., Martin, M. E., McDowell, W. H., Melillo,
 1089 J. M. and Steudler, P.: Ecosystem response to 15 years of chronic nitrogen additions at the
 1090 Harvard Forest LTER, Massachusetts, USA, *Forest Ecology and Management*, 196(1), 7–28,
 1091 doi:10.1016/j.foreco.2004.03.033, 2004.
- 1092 Mäkelä, A., Valentine, H. T. and Helmisaari, H.-S.: Optimal co-allocation of carbon and nitrogen
 1093 in a forest stand at steady state, *New Phytologist*, 180(1), 114–123, doi:10.1111/j.1469-
 1094 8137.2008.02558.x, 2008.
- 1095 Martin, A. R., Gezahegn, S. and Thomas, S. C.: Variation in carbon and nitrogen concentration
 1096 among major woody tissue types in temperate trees, *Can. J. For. Res.*, 45(6), 744–757,
 1097 doi:10.1139/cjfr-2015-0024, 2015.
- 1098 McDowell, N., Barnard, H., Bond, B., Hinckley, T., Hubbard, R., Ishii, H., Köstner, B., Magnani, F.,
 1099 Marshall, J., Meinzer, F., Phillips, N., Ryan, M. and Whitehead, D.: The relationship between
 1100 tree height and leaf area: sapwood area ratio, *Oecologia*, 132(1), 12–20, doi:10.1007/s00442-
 1101 002-0904-x, 2002.
- 1102 McGill, B. J. and Brown, J. S.: Evolutionary Game Theory and Adaptive Dynamics of Continuous
 1103 Traits, *Annual Review of Ecology, Evolution, and Systematics*, 38(1), 403–435,
 1104 doi:10.1146/annurev.ecolsys.36.091704.175517, 2007.
- 1105 McMurtrie, R. E., Iversen, C. M., Dewar, R. C., Medlyn, B. E., Näsholm, T., Pepper, D. A. and
 1106 Norby, R. J.: Plant root distributions and nitrogen uptake predicted by a hypothesis of optimal
 1107 root foraging, *Ecology and Evolution*, 2(6), 1235–1250, doi:10.1002/ece3.266, 2012.
- 1108 McNickle, G. G. and Brown, J. S.: An ideal free distribution explains the root production of
 1109 plants that do not engage in a tragedy of the commons game, edited by S. Schwinning, *Journal*
 1110 *of Ecology*, 102(4), 963–971, doi:10.1111/1365-2745.12259, 2014.
- 1111 McNickle, G. G. and Dybzinski, R.: Game theory and plant ecology, edited by J. Klironomos,
 1112 *Ecology Letters*, 16(4), 545–555, doi:10.1111/ele.12071, 2013.
- 1113 Melillo, J. M., Butler, S., Johnson, J., Mohan, J., Steudler, P., Lux, H., Burrows, E., Bowles, F.,
 1114 Smith, R., Scott, L., Vario, C., Hill, T., Burton, A., Zhou, Y.-M. and Tang, J.: Soil warming, carbon-
 1115 nitrogen interactions, and forest carbon budgets, *Proceedings of the National Academy of*
 1116 *Sciences*, 108(23), 9508–9512, doi:10.1073/pnas.1018189108, 2011.

- 1117 Menge, D. N. L., Batterman, S. A., Hedin, L. O., Liao, W., Pacala, S. W. and Taylor, B. N.: Why are
 1118 nitrogen-fixing trees rare at higher compared to lower latitudes?, *Ecology*, 98(12), 3127–3140,
 1119 doi:10.1002/ecy.2034, 2017.
- 1120 Michelot, A., Simard, S., Rathgeber, C., Dufrene, E. and Damesin, C.: Comparing the intra-annual
 1121 wood formation of three European species (*Fagus sylvatica*, *Quercus petraea* and *Pinus*
 1122 *sylvestris*) as related to leaf phenology and non-structural carbohydrate dynamics, *Tree*
 1123 *Physiology*, 32(8), 1033–1045, doi:10.1093/treephys/tps052, 2012.
- 1124 Montané, F., Fox, A. M., Arellano, A. F., MacBean, N., Alexander, M. R., Dye, A., Bishop, D. A.,
 1125 Trouet, V., Babst, F., Hessler, A. E., Pederson, N., Blanken, P. D., Bohrer, G., Gough, C. M., Litvak,
 1126 M. E., Novick, K. A., Phillips, R. P., Wood, J. D. and Moore, D. J. P.: Evaluating the effect of
 1127 alternative carbon allocation schemes in a land surface model (CLM4.5) on carbon fluxes, pools,
 1128 and turnover in temperate forests, *Geoscientific Model Development*, 10(9), 3499–3517,
 1129 doi:10.5194/gmd-10-3499-2017, 2017.
- 1130 Moorcroft, P. R., Hurtt, G. C. and Pacala, S. W.: A method for scaling vegetation dynamics: The
 1131 ecosystem demography model (ED), *Ecological Monographs*, 71(4), 557–585, doi:10.1890/0012-
 1132 9615(2001)071[0557:AMFSVD]2.0.CO;2, 2001.
- 1133 Morris, E. C., Griffiths, M., Golebiowska, A., Mairhofer, S., Burr-Hersey, J., Goh, T., Wangenheim,
 1134 D. von, Atkinson, B., Sturrock, C. J., Lynch, J. P., Vissenberg, K., Ritz, K., Wells, D. M., Mooney, S.
 1135 J. and Bennett, M. J.: Shaping 3D Root System Architecture, *Current Biology*, 27(17), R919–
 1136 R930, doi:10.1016/j.cub.2017.06.043, 2017.
- 1137 Nie, M., Lu, M., Bell, J., Raut, S. and Pendall, E.: Altered root traits due to elevated CO₂: a meta-
 1138 analysis: Root traits at elevated CO₂, *Global Ecology and Biogeography*, 22(10), 1095–1105,
 1139 doi:10.1111/geb.12062, 2013.
- 1140 Norby, R. J. and Zak, D. R.: Ecological Lessons from Free-Air CO₂ Enrichment (FACE)
 1141 Experiments, *Annual Review of Ecology, Evolution, and Systematics*, 42(1), 181–203,
 1142 doi:10.1146/annurev-ecolsys-102209-144647, 2011.
- 1143 Norby, R. J., Sholtis, J. D., Gunderson, C. A. and Jawdy, S. S.: Leaf dynamics of a deciduous forest
 1144 canopy: no response to elevated CO₂, *Oecologia*, 136(4), 574–584, doi:10.1007/s00442-003-
 1145 1296-2, 2003.
- 1146 O’Brien, E. E., Gersani, M. and Brown, J. S.: Root proliferation and seed yield in response to
 1147 spatial heterogeneity of below-ground competition, *New Phytologist*, 168(2), 401–412,
 1148 doi:10.1111/j.1469-8137.2005.01520.x, 2005.
- 1149 Ordoñez, J. C., van Bodegom, P. M., Witte, J.-P. M., Wright, I. J., Reich, P. B. and Aerts, R.: A
 1150 global study of relationships between leaf traits, climate and soil measures of nutrient fertility,
 1151 *Global Ecology and Biogeography*, 18(2), 137–149, doi:10.1111/j.1466-8238.2008.00441.x,
 1152 2009.

- 1153 Oyewole, O. A., Inselsbacher, E., Näsholm, T. and Jämtgård, S.: Incorporating mass flow strongly
 1154 promotes N flux rates in boreal forest soils, *Soil Biology and Biochemistry*, 114, 263–269,
 1155 doi:10.1016/j.soilbio.2017.07.021, 2017.
- 1156 Pappas, C., Fatichi, S. and Burlando, P.: Modeling terrestrial carbon and water dynamics across
 1157 climatic gradients: does plant trait diversity matter?, *New Phytologist*, 209(1), 137–151,
 1158 doi:10.1111/nph.13590, 2016.
- 1159 Parton, W., Schimel, D., Cole, C. and Ojima, D.: Analysis of factors controlling soil organic matter
 1160 levels in Great Plains grasslands, *Soil Science Society of America Journal*, 51(5), 1173–1179,
 1161 doi:10.2136/sssaj1987.03615995005100050015x, 1987.
- 1162 Phillips, R. P., Finzi, A. C. and Bernhardt, E. S.: Enhanced root exudation induces microbial
 1163 feedbacks to N cycling in a pine forest under long-term CO₂ fumigation, *Ecology Letters*, 14(2),
 1164 187–194, doi:10.1111/j.1461-0248.2010.01570.x, 2011.
- 1165 Phillips, R. P., Brzostek, E. and Midgley, M. G.: The mycorrhizal-associated nutrient economy: a
 1166 new framework for predicting carbon-nutrient couplings in temperate forests, *New Phytologist*,
 1167 199(1), 41–51, doi:10.1111/nph.12221, 2013.
- 1168 Plomion, C., Leprovost, G. and Stokes, A.: Wood Formation in Trees, *PLANT PHYSIOLOGY*,
 1169 127(4), 1513–1523, doi:10.1104/pp.010816, 2001.
- 1170 Poorter, H., Niklas, K. J., Reich, P. B., Oleksyn, J., Poot, P. and Mommer, L.: Biomass allocation to
 1171 leaves, stems and roots: meta-analyses of interspecific variation and environmental control:
 1172 Tansley review, *New Phytologist*, 193(1), 30–50, doi:10.1111/j.1469-8137.2011.03952.x, 2012.
- 1173 Post, W. M., Pastor, J., Zinke, P. J. and Stangenberger, A. G.: Global patterns of soil nitrogen
 1174 storage, *Nature*, 317(6038), 613–616, doi:10.1038/317613a0, 1985.
- 1175 Pregitzer, K. S., Hendrick, R. L. and Fogel, R.: The demography of fine roots in response to
 1176 patches of water and nitrogen, *New Phytologist*, 125(3), 575–580, doi:10.1111/j.1469-
 1177 8137.1993.tb03905.x, 1993.
- 1178 Pregitzer, K. S., DeForest, J. L., Burton, A. J., Allen, M. F., Ruess, R. W. and Hendrick, R. L.: Fine
 1179 Root Architecture of Nine North American Trees, *Ecological Monographs*, 72(2), 293,
 1180 doi:10.2307/3100029, 2002.
- 1181 Raich, J., Rastetter, E. B., Melillo, J. M., Kicklighter, D. W., Steudler, P. A., Peterson, B. J., Grace,
 1182 A., Moore, B. and Vorosmary, C. J.: Potential Net Primary Productivity in South America:
 1183 Application of a Global Model, *Ecological Applications*, 1(4), 399–429, doi:10.2307/1941899,
 1184 1991.
- 1185 Randerson, J., Thompson, M., Conway, T., Fung, I. and Field, C.: The contribution of terrestrial
 1186 sources and sinks to trends in the seasonal cycle of atmospheric carbon dioxide, *Global
 1187 Biogeochemical Cycles*, 11(4), 535–560, doi:10.1029/97GB02268, 1997.

- 1188 Reich, P. B., Luo, Y., Bradford, J. B., Poorter, H., Perry, C. H. and Oleksyn, J.: Temperature drives
1189 global patterns in forest biomass distribution in leaves, stems, and roots, *Proceedings of the*
1190 *National Academy of Sciences*, 111(38), 13721–13726, doi:10.1073/pnas.1216053111, 2014.
- 1191 Savage, K. E., Parton, W. J., Davidson, E. A., Trumbore, S. E. and Frey, S. D.: Long-term changes
1192 in forest carbon under temperature and nitrogen amendments in a temperate northern
1193 hardwood forest, *Global Change Biology*, 19(8), 2389–2400, doi:10.1111/gcb.12224, 2013.
- 1194 Scheiter, S. and Higgins, S. I.: Impacts of climate change on the vegetation of Africa: an adaptive
1195 dynamic vegetation modelling approach, *Global Change Biology*, 15(9), 2224–2246,
1196 doi:10.1111/j.1365-2486.2008.01838.x, 2009.
- 1197 Scheiter, S., Langan, L. and Higgins, S. I.: Next-generation dynamic global vegetation models:
1198 learning from community ecology, *New Phytologist*, 198(3), 957–969, doi:10.1111/nph.12210,
1199 2013.
- 1200 Schmidt, G. A., Kelley, M., Nazarenko, L., Ruedy, R., Russell, G. L., Aleinov, I., Bauer, M., Bauer,
1201 S. E., Bhat, M. K., Bleck, R., Canuto, V., Chen, Y.-H., Cheng, Y., Clune, T. L., Del Genio, A., de
1202 Fainchtein, R., Faluvegi, G., Hansen, J. E., Healy, R. J., Kiang, N. Y., Koch, D., Lacis, A. A.,
1203 LeGrande, A. N., Lerner, J., Lo, K. K., Matthews, E. E., Menon, S., Miller, R. L., Oinas, V., Oloso, A.
1204 O., Perlwitz, J. P., Puma, M. J., Putman, W. M., Rind, D., Romanou, A., Sato, M., Shindell, D. T.,
1205 Sun, S., Syed, R. A., Tausnev, N., Tsigaridis, K., Unger, N., Voulgarakis, A., Yao, M.-S. and Zhang,
1206 J.: Configuration and assessment of the GISS ModelE2 contributions to the CMIP5 archive,
1207 *Journal of Advances in Modeling Earth Systems*, 6(1), 141–184, doi:10.1002/2013MS000265,
1208 2014.
- 1209 Shevliakova, E., Pacala, S. W., Malyshev, S., Hurtt, G. C., Milly, P. C. D., Caspersen, J. P.,
1210 Sentman, L. T., Fisk, J. P., Wirth, C. and Crevoisier, C.: Carbon cycling under 300 years of land
1211 use change: Importance of the secondary vegetation sink, *Global Biogeochemical Cycles*, 23,
1212 GB2022, doi:10.1029/2007GB003176, 2009.
- 1213 Shinozaki, Kichiro, Yoda, Kyoji, Hozumi, Kazuo and Kira, Tatu: A quantitative analysis of plant
1214 form – the pipe model theory. I. Basic analyses, *Japanese Journal of Ecology*, 14(3), 97–105,
1215 1964.
- 1216 Sierra, C. A. and Mueller, M.: A general mathematical framework for representing soil organic
1217 matter dynamics, *Ecological Monographs*, 85(4), 505–524, doi:10.1890/15-0361.1, 2015.
- 1218 Sierra, C. A., Muller, M., Metzler, H., Manzoni, S. and Trumbore, S. E.: The muddle of ages,
1219 turnover, transit, and residence times in the carbon cycle, *Global Change Biology*, 23(5), 1763–
1220 1773, doi:10.1111/gcb.13556, 2017.
- 1221 Sitch, S., Smith, B., Prentice, I. C., Arneth, A., Bondeau, A., Cramer, W., Kaplan, J. O., Levis, S.,
1222 Lucht, W., Sykes, M. T., Thonicke, K. and Venevsky, S.: Evaluation of ecosystem dynamics, plant

- 1223 geography and terrestrial carbon cycling in the LPJ dynamic global vegetation model, *Global*
1224 *Change Biology*, 9(2), 161–185, doi:10.1046/j.1365-2486.2003.00569.x, 2003.
- 1225 Smith, A. R., Lukac, M., Bambrick, M., Miglietta, F. and Godbold, D. L.: Tree species diversity
1226 interacts with elevated CO₂ to induce a greater root system response, *Glob Change Biol*, 19(1),
1227 217–228, doi:10.1111/gcb.12039, 2013.
- 1228 Soriano, D., Orozco-Segovia, A., Márquez-Guzmán, J., Kitajima, K., Gamboa-de Buen, A. and
1229 Huante, P.: Seed reserve composition in 19 tree species of a tropical deciduous forest in Mexico
1230 and its relationship to seed germination and seedling growth, *Annals of Botany*, 107(6), 939–
1231 951, doi:10.1093/aob/mcr041, 2011.
- 1232 Strigul, N., Pristinski, D., Purves, D., Dushoff, J. and Pacala, S.: Scaling from trees to forests:
1233 tractable macroscopic equations for forest dynamics, *Ecological Monographs*, 78(4), 523–545,
1234 doi:10.1890/08-0082.1, 2008.
- 1235 Sulman, B. N., Phillips, R. P., Oishi, A. C., Shevliakova, E. and Pacala, S. W.: Microbe-driven
1236 turnover offsets mineral-mediated storage of soil carbon under elevated CO₂, *Nature Climate*
1237 *Change*, 4(12), 1099–1102, doi:10.1038/NCLIMATE2436, 2014.
- 1238 Terrer, C., Vicca, S., Hungate, B. A., Phillips, R. P. and Prentice, I. C.: Mycorrhizal association as a
1239 primary control of the CO₂ fertilization effect, *Science*, 353(6294), 72–74,
1240 doi:10.1126/science.aaf4610, 2016.
- 1241 Terrer, C., Vicca, S., Stocker, B. D., Hungate, B. A., Phillips, R. P., Reich, P. B., Finzi, A. C. and
1242 Prentice, I. C.: Ecosystem responses to elevated CO₂ governed by plant-soil interactions and the
1243 cost of nitrogen acquisition, *New Phytol*, 217(2), 507–522, doi:10.1111/nph.14872, 2018.
- 1244 Tilman, D.: *Plant strategies and the dynamics and structure of plant communities*, Princeton
1245 University Press, Princeton, N.J., 1988.
- 1246 Urbanski, S., Barford, C., Wofsy, S., Kucharik, C., Pyle, E., Budney, J., McKain, K., Fitzjarrald, D.,
1247 Czikowsky, M. and Munger, J. W.: Factors controlling CO₂ exchange on timescales from hourly
1248 to decadal at Harvard Forest, *Journal of Geophysical Research - Biogeosciences*, 112(G2),
1249 doi:10.1029/2006JG000293, 2007.
- 1250 Valentine, H. T. and Mäkelä, A.: Modeling forest stand dynamics from optimal balances of
1251 carbon and nitrogen, *New Phytologist*, 194(4), 961–971, doi:10.1111/j.1469-
1252 8137.2012.04123.x, 2012.
- 1253 Vitousek, P. M., Menge, D. N. L., Reed, S. C. and Cleveland, C. C.: Biological nitrogen fixation:
1254 rates, patterns and ecological controls in terrestrial ecosystems, *Philosophical Transactions of*
1255 *the Royal Society B: Biological Sciences*, 368(1621), 20130119–20130119,
1256 doi:10.1098/rstb.2013.0119, 2013.

- 1257 Walker, A. P., De Kauwe, M. G., Medlyn, B. E., Zaehle, S., Iversen, C. M., Asao, S., Guenet, B.,
1258 Harper, A., Hickler, T., Hungate, B. A., Jain, A. K., Luo, Y., Lu, X., Lu, M., Luus, K., Megonigal, J. P.,
1259 Oren, R., Ryan, E., Shu, S., Talhelm, A., Wang, Y.-P., Warren, J. M., Werner, C., Xia, J., Yang, B.,
1260 Zak, D. R. and Norby, R. J.: Decadal biomass increment in early secondary succession woody
1261 ecosystems is increased by CO₂ enrichment, *Nat Commun*, 10(1), 454, doi:10.1038/s41467-019-
1262 08348-1, 2019.
- 1263 Weng, E., Farris, C. E., Dybzinski, R. and Pacala, S. W.: Predicting vegetation type through
1264 physiological and environmental interactions with leaf traits: evergreen and deciduous forests
1265 in an earth system modeling framework, *Global Change Biology*, 23(6), 2482–2498,
1266 doi:10.1111/gcb.13542, 2017.
- 1267 Weng, E. S., Malyshev, S., Lichstein, J. W., Farris, C. E., Dybzinski, R., Zhang, T., Shevliakova, E.
1268 and Pacala, S. W.: Scaling from individual trees to forests in an Earth system modeling
1269 framework using a mathematically tractable model of height-structured competition,
1270 *Biogeosciences*, 12(9), 2655–2694, doi:10.5194/bg-12-2655-2015, 2015.
- 1271 Wieder, W. R., Grandy, A. S., Kallenbach, C. M. and Bonan, G. B.: Integrating microbial
1272 physiology and physio-chemical principles in soils with the Microbial-Mineral Carbon
1273 Stabilization (MIMICS) model, *BIOGEOSCIENCES*, 11(14), 3899–3917, doi:10.5194/bg-11-3899-
1274 2014, 2014.
- 1275 Wieder, W. R., Allison, S. D., Davidson, E. A., Georgiou, K., Hararuk, O., He, Y., Hopkins, F., Luo,
1276 Y., Smith, M. J., Sulman, B., Todd-Brown, K., Wang, Y.-P., Xia, J. and Xu, X.: Explicitly
1277 representing soil microbial processes in Earth system models, *GLOBAL BIOGEOCHEMICAL*
1278 *CYCLES*, 29(10), 1782–1800, doi:10.1002/2015GB005188, 2015.
- 1279 Wright, I., Reich, P., Westoby, M., Ackerly, D., Baruch, Z., Bongers, F., Cavender-Bares, J.,
1280 Chapin, T., Cornelissen, J., Diemer, M., Flexas, J., Garnier, E., Groom, P., Gulias, J., Hikosaka, K.,
1281 Lamont, B., Lee, T., Lee, W., Lusk, C., Midgley, J., Navas, M., Niinemets, U., Oleksyn, J., Osada,
1282 N., Poorter, H., Poot, P., Prior, L., Pyankov, V., Roumet, C., Thomas, S., Tjoelker, M., Veneklaas,
1283 E. and Villar, R.: The worldwide leaf economics spectrum, *NATURE*, 428(6985), 821–827,
1284 doi:10.1038/nature02403, 2004.
- 1285 Xia, J., Luo, Y., Wang, Y.-P. and Hararuk, O.: Traceable components of terrestrial carbon storage
1286 capacity in biogeochemical models, *Global Change Biology*, 19(7), 2104–2116,
1287 doi:10.1111/gcb.12172, 2013.
- 1288 Yang, Y., Luo, Y. and Finzi, A. C.: Carbon and nitrogen dynamics during forest stand
1289 development: a global synthesis, *New Phytologist*, 190(4), 977–989, doi:10.1111/j.1469-
1290 8137.2011.03645.x, 2011.
- 1291 Zadworny, M., McCormack, M. L., Mucha, J., Reich, P. B. and Oleksyn, J.: Scots pine fine roots
1292 adjust along a 2000-km latitudinal climatic gradient, *New Phytologist*, 212(2), 389–399,
1293 doi:10.1111/nph.14048, 2016.

1294 Zea-Cabrera, E., Iwasa, Y., Levin, S. and Rodríguez-Iturbe, I.: Tragedy of the commons in plant
1295 water use, *Water Resources Research*, 42(6), W06D02, doi:10.1029/2005WR004514, 2006.
1296